



U.S. DEPARTMENT OF
ENERGY

PNNL-18820

Prepared for the U.S. Department of Energy
under Contract DE-AC05-76RL01830

PNNL Fungal Biotechnology Core DOE-OBP Project

SE Baker
KS Bruno
MG Butcher

JR Collett
DE Culley
Z Dai

JK Magnuson
EA Panisko

November 2009



Pacific Northwest
NATIONAL LABORATORY

*Proudly Operated by **Battelle** Since 1965*

DISCLAIMER

This report was prepared as an account of work sponsored by an agency of the United States Government. Neither the United States Government nor any agency thereof, nor Battelle Memorial Institute, nor any of their employees, makes **any warranty, express or implied, or assumes any legal liability or responsibility for the accuracy, completeness, or usefulness of any information, apparatus, product, or process disclosed, or represents that its use would not infringe privately owned rights.** Reference herein to any specific commercial product, process, or service by trade name, trademark, manufacturer, or otherwise does not necessarily constitute or imply its endorsement, recommendation, or favoring by the United States Government or any agency thereof, or Battelle Memorial Institute. The views and opinions of authors expressed herein do not necessarily state or reflect those of the United States Government or any agency thereof.

PACIFIC NORTHWEST NATIONAL LABORATORY
operated by
BATTELLE
for the
UNITED STATES DEPARTMENT OF ENERGY
under Contract DE-ACO5-76RL01830

Printed in the United States of America

**Available to DOE and DOE contractors from the
Office of Scientific and Technical Information,
P.O. Box 62, Oak Ridge, TN 37831-0062;
ph: (865) 576-8401
fax: (865) 576 5728
email: reports@adonis.osti.gov**

**Available to the public from the National Technical Information Service,
U.S. Department of Commerce, 5285 Port Royal Rd., Springfield, VA 22161
ph: (800) 553-6847
fax: (703) 605-6900
email: orders@nits.fedworld.gov
online ordering: <http://www.ntis.gov/ordering.htm>**

PNNL Fungal Biotechnology Core DOE-OBP Project

SE Baker
KS Bruno
MG Butcher

JR Collett
DE Culley
Z Dai

JK Magnuson
EA Panisko

November 2009

Prepared for
the U.S. Department of Energy
under Contract DE-AC05-76RL01830

Pacific Northwest National Laboratory
Richland, Washington 99352

Summary

In 2009, we continued to address barriers to fungal fermentation in the primary areas of morphology control, genomics, proteomics, fungal hyperproductivity, biomass-to-products via fungal based consolidated bioprocesses, and filamentous fungal ethanol. “Alternative renewable fuels from fungi” was added as a new subtask. Plans were also made to launch a new advanced strain development subtask in FY2010. Project subtask highlights included:

- **Morphology:** Key accomplishments included analysis of genes involved in control of fungal bioprocess organism morphology and a morphology scoring system for quantitative measurement. This task was closed out and replaced beginning in FY10 with **Advanced Strain Development**.
- **Genomics:** Tools for generating defined marker genes and improved throughput gene deletions were developed. Gene expression constructs and strategies were also developed. Genetic analysis of genes identified through functional genomic studies as important for fungal bioprocesses was performed.
- **Proteomics:** Proteomic analysis of productive and non-productive fungal bioprocesses led to the identification of proteins and associated genes for follow-up analysis.
- **Hyper-productivity and consolidated bioprocesses:** Excellent progress was made towards understanding the biosynthesis of itaconic acid. *Trichoderma reesei* and *Aspergillus terreus* bioprocesses were baselined.
- **Filamentous fungal ethanol:** Flux modeling was used to understand *Aspergillus oryzae* pentose utilization and ethanol production. A number of deletion strains were made in *A. oryzae*.
- **Alternative renewable fuels from fungi:** We have explored possible fungal routes to next-generation renewable fuels—beyond ethanol.
- **Advanced Strain Development:** In FY 10, initiating the development of a core capability aimed at generating fungal strains with improved enzyme, biofuel, and organic acid secretion.

Acknowledgments

We want to thank the U.S. Department of Energy Office of the Biomass Program for its continued financial support of this research project. We also want to thank the members of the industrial Partners Review Board (Novozymes, Inc., POET Energy, Inc., Verenum, Inc., Mycosynthetix, Inc., and Dyadic International) for providing their real-world perspectives to our project.

Acronyms and Abbreviations

ATP	adenosine tri-phosphate
BSEL	Bioproducts, Sciences, and Engineering Laboratory
CAP	citric acid production (medium)
COBRA	Constraint-Based Reconstruction and Analysis
DO	dissolved oxygen
DOE	U.S. Department of Energy
DOE-SC	U.S. Department of Energy Office of Science
DTU	Technical University of Denmark
EST	expressed sequence tag
FBA	flux balance analysis
FOA	5-Fluoroorotic Acid
GFP	green fluorescent protein
GUS	glucuronidase
HPLC	high-performance liquid chromatography
IMP	<u>I</u> mpedes <u>M</u> itogenic signal <u>P</u> ropagation
JBEI	Joint BioEnergy Institute
JGI	Joint Genome Institute
LC	liquid chromatography
LDRD	Laboratory Directed Research and Development
MFS	major facilitator superfamily
MS	mass spectrometry
NMR	nuclear magnetic resonance
PCR	polymerase chain reaction
PKS	polyketide synthase
PNNL	Pacific Northwest National Laboratory
PPIB	peptidyl-prolyl cis-trans isomerase B
PRB	Partner Review Board
ROS	reactive oxygen species
SBML	System Biology Markup Language
SDM	sulfate depleted medium
SSF	simultaneous saccharification and fermentation
SSH	suppressive subtractive hybridization
WDG	wet distillers grains

Contents

Summary	iii
Acknowledgments.....	v
Acronyms and Abbreviations	vii
1.0 Introduction	1.1
2.0 Major Subtask A.1: Morphology Control Technology.....	2.1
2.1 Background	2.1
2.2 Accomplishments and Results	2.1
2.3 Plans for FY10	2.4
3.0 Major Subtask A.2 Fungal Genomics.....	3.1
3.1 Background	3.1
3.2 Objectives.....	3.2
3.3 Accomplishments and Results	3.2
3.4 Plans for FY2010	3.5
4.0 Major Subtask A.3 Fungal Proteomics.....	4.1
4.1 Background	4.1
4.2 Accomplishments and Results	4.1
4.3 Plans for FY2010	4.8
5.0 Major Subtask A.4a Fungal Hyperproductivity.....	5.1
5.1 Background	5.1
5.2 Accomplishments and Results	5.2
5.3 Plans for FY2010	5.3
6.0 Major Subtask A.4b Consolidated Bioprocesses.....	6.1
6.1 Background	6.1
6.1.1 Specific Objectives.....	6.1
6.2 Accomplishments and Results	6.1
6.3 Plans for FY2010	6.3
7.0 Major Subtask A.5 Alternative Fungal Ethanologen Characterization and Metabolic Model Analysis	7.1
7.1 Background	7.1
7.2 Accomplishments and Results	7.1
7.2.1 Metabolic Modeling.....	7.1
7.2.2 Fermentation.....	7.3
7.3 Plans for FY2010	7.11

8.0 Major Subtask A.6 Alternative Renewable Fuels from Fungi.....	8.1
8.1 Background.....	8.1
8.2 Accomplishments and Results.....	8.1
8.3 Plans for FY10.....	8.3
9.0 References.....	9.1
10.0 Publications.....	10.1
Appendix A: Complete Analysis Report.....	A.1

Figures

2.1. Scoring System for Fungal Morphology.....	2.3
2.2. MapK1 Mutant Morphology Score.....	2.3
2.3. GFP as a Tool for Marking Tips.....	2.4
3.1. Mutation of ATP Sulfurylase in <i>A. Niger</i>	3.4
3.2. Improved Homologous Recombination in the <i>kusA</i> Mutant.....	3.5
3.3. The Percent Viability of Wildtype, <i>kusA</i> ⁻ , and <i>kusA</i> ⁺ Revertant Spores Exposed to Gamma Radiation.....	3.6
3.4. Phenotype Screen of Five Mutants (six colonies each) on CAP Media.....	3.7
4.1. Phytase Assays on Phytase from Wheat and Cell Lysates and Spent Media from <i>A. niger</i> Grown Under Filamentous (+ Mn) and Pelleted Conditions (no Mn).....	4.4
4.2. Protein Sequence Alignment of JGI Gene Model 213198 and Human Cyclophilins.....	4.5
4.3. Anti-Cyclophilin Western Analysis to Identify Expression of JGI Gene Model 213198 from Cell Extracts of Filamentous (+ Mn) and Pelleted (-Mn) from <i>A. niger</i> Cultures.....	4.6
5.1. 20-L Fermentation of Glucose to Itaconic Acid by <i>Aspergillus terreus</i>	5.2
5.2. Snapshot of the <i>Aspergillus terreus</i> Chromosome Region Containing the Lovastatin and Itaconic Acid Gene Clusters.....	5.3
6.1. Enzyme activities in <i>Trichoderma reesei</i> QM6a Grown on Cellulose.....	6.2
7.1. (Left chart) Ethanol Output Flux Changes Predicted from FBA of <i>A. Oryzae</i> Cellular Metabolism as a Function of Oxygen Uptake Flux.....	7.3
7.2. Ethanol Responsive Promoters from the <i>E. coli</i> Genes <i>dnaK</i> , <i>grpE</i> , <i>katG</i> , <i>pgaA</i> , and <i>uspA</i> Fused with Reporter Gene LacZ-Alpha in a pBS KS (+) Plasmid Background, Sequenced and Transformed into <i>E. Coli</i>	7.5
7.3. Exp 40, <i>A. oryzae</i> NRRL 697, <i>alcR</i> and <i>creA</i> Mutants Ethanol Production on 12% Glucose Minimal Medium Enriched with 0.5% Yeast Extract (averages for nine replicates).....	7.7
7.4. Exp 42, <i>A. oryzae</i> NRRL 697, <i>alcR</i> and <i>creA</i> Mutants Comparison for Ethanol Production on 12% Xylose Minimal Medium Enriched with 0.5% Yeast Extract (averages for nine replicates).....	7.7

7.5.	Exp 51, <i>Aspergillus oryzae</i> NRRL 697 Model Strain Ethanol Production on 12% Glucose Minimal Medium Enriched with 0.5% Yeast Extract, 20-Liter Working Volume, and 2×10^7 Spores/mL	7.8
7.6.	Exp 49, <i>A. oryzae</i> NRRL 697 Model Strain on Ethanol Production on 12% Glucose Minimal Medium Enriched with 0.5% Yeast Extract, 20-Liter Working Volume, and 2×10^7 Spores/mL	7.9
7.7.	Exp 46, Xylitol Remaining from <i>A. oryzae</i> NRRL 697 Model Strain on 4% Xylitol Minimal Medium Enriched with 0.5% Yeast Extract, 250-mL flasks, 100 mL of working volume, and 2×10^7 spores/mL	7.10
7.8.	Exp 44, <i>A. oryzae</i> NRRL 697 Model Strain Ethanol Production on 12% Glucose Minimal Medium Enriched with 0.5% Yeast Extract, or 10 % Source 1 Thin Stillage or 10% Source 2 Thin Stillage, 250-mL flasks, 100 mL of working volume, and 2×10^7 spores/mL ...	7.10
7.9.	Exp 44, <i>A. oryzae</i> NRRL 697 Model Strain Ethanol Production on 12% Xylose Minimal Medium Enriched with 0.5% Yeast Extract, or 10% Source 1(S1) Thin Stillage or 10% Source 2 (S2) Thin Stillage, 250-mL flasks, 100 mL of Working Volume, and 2×10^7 spores/mL	7.11

Tables

3.1.	Fungal Expression Constructs	3.2
3.2.	Genetic Markers Available for Gene Manipulation in Relevant Strains	3.4
4.1.	Proteins Higher in Abundance in the Filamentous vs. Pelleted Growth State	4.2
4.2.	Proteins Higher in Abundance in the Pelleted vs. Filamentous Growth State	4.3
4.3.	A Summary of Identifications from Affinity-Purified Ubiquitin	4.7
8.1.	Classes of Hydrocarbon and Hydrocarbon-Like Molecules Produced by Fungi	8.1

1.0 Introduction

The research of the Pacific Northwest National Laboratory (PNNL) Fungal Biotechnology Team is focused on generating an in-depth understanding of the biological processes underlying efficient fungal bioprocesses whose end products are fuels, organic acids, and enzymes. The fundamental and practical knowledge and tools that we generate will improve the efficiency and ease of implementing fungal biotechnology in industry and lead to more rapid and effective development of new processes for the biorefinery industry.

Improved fungal biotechnology tools will be very important for establishing bioprocesses within integrated biorefineries. Fungi have the potential for a rapid, highly productive conversion of biomass resources to bio-based products and intermediates that bring economic benefit to the biorefinery industry. While fungal fermentations are currently used to produce a limited number of specialized products, the tools for broader and more rapid implementation of fungal-based production processes are needed for this industry. Moreover, many of the current fungal processes in use have been developed over many years without a clear understanding of the underlying biological mechanisms that allow the control and utilization of fungal organisms.

The overarching goal of this project is to generate innovative fungal-based biotechnology to enable a robust biorefinery industry. The project objectives are to:

- Reduce the cost of biofuels and bioproducts
 - Directly utilize complex biomass
 - Enable processes with high concentrations of end-products (e.g., fuels, organic acids, and enzymes)
- Improve technology for engineering filamentous fungi
- Leverage industry needs and expertise to help guide the research program.

To achieve the objectives of creating tools that enable an economically viable biorefinery using fungal biotechnology, the research has been divided into six major technical subtasks.

- Morphology control
- Genomics
- Proteomics
- Hyper-productivity and consolidated bioprocesses
- Filamentous fungal ethanol
- Alternative renewable fuels from fungi.

The research conducted during FY2009 in these focus areas and research plans for FY2010 are presented in this report.

2.0 Major Subtask A.1: Morphology Control Technology

2.1 Background

Proper morphology in filamentous fungi is known to be associated with highly productive bioprocesses for making small metabolites (fuels and chemicals) and enzymes. Therefore, genetically controlling morphology in filamentous fungi will ultimately lead to increased productivity and improved bioprocess efficiency. The genetics of morphology control in filamentous fungi is being examined using *Aspergillus niger* and citric acid production as our primary model system. Genes that are identified in *A.niger* will be examined for effectiveness in controlling morphology in our second model system, *Aspergillus terreus* and itaconic acid production. The ultimate goal is to control the morphology in any fungus that makes a fuel or product of interest. The research conducted under this subtask is focused on identifying genes that can be manipulated to induce a pelleted morphology and an accompanying model that provides a framework for understanding morphology control in filamentous fungi.

Our current morphology control model provides a system-level explanation. These systems include the G protein system, the Ras signaling system, the ubiquitin system, and the reactive oxygen species (ROS) response system.

2.2 Accomplishments and Results

In FY09, we continued our research efforts on the three systems mentioned above. In the G protein system, three additional G protein-coupled genes were deleted. Thus far, we have deleted all G protein subunits ($G\alpha 1$, $G\alpha 2$, $G\alpha 3$, $G\beta$ and $G\gamma$), 10 G protein-coupled receptors (GprA, GprB, GprC, GprD, GprE, GprF, GprH, GprM, GprN, GprP). Among those deleted genes in the G protein system, we found that $G\alpha 1$, $G\beta$, and GprB have notable effects on fungal growth and development. In the Ras regulatory system, the Impedes Mitogenic signal Propagation (IMP), which inhibits the functional coupling between Raf and MEKkinases of the Raf-MEK-ERK scaffolding protein KSR1, was identified with the T-DNA insertion with the first exon of the IMP gene via *Agrobacterium*-mediated transformation. The interruption of the IMP gene has a dramatic effect on *A. niger* morphology and asexual sporulation. To further examine the function of the IMP gene, we created a gene-deletion construct and an affinity-tag fusion for transformation into *A. niger*. The mutants with IMP deletion or affinity-tagging were generated. The confirmation and isolation of those proteins associated with the IMP are underway.

The ubiquitin protein system exerts its functions by ubiquitinating the targeting proteins for degradation, protein compartmentation, or temporal regulation. Three approaches have been employed to further understand how the ubiquitin protein system is involved in *A. niger* morphology. First, those ubiquitinated proteins should be identified via affinity-tagging purification. The second one is to delete the selected genes to examine their contribution in fungal morphology. The final one is to conditionally express the ubiquitin or ubiquitinated proteins in fungi to determine their potential effects on fungal morphology and chemical or protein production. The ubiquitinated proteins were purified from *A. niger* biomass of either filamentous or pelleted growth by affinity purification. The ubiquitinated proteins were determined by liquid chromatography-mass spectrometry (LC-MS). Some of ubiquitinated proteins identified from either filamentous or pelleted growth were selected for gene deletion. Ten oligo

nucleotides were designed and de novo synthesized, and gene-deletion construction, transformation, and characterization are ongoing. In addition, three ubiquitin-specific proteases and two SUMO-specific proteases were deleted, and their effects on fungal morphology are being examined.

To conditionally express a selected gene, two inducible promoters (nitrate reductase [*niaD*] promoter and Adenosine Triphosphate (ATP) sulfurylase [*met3*] promoter) were selected. Since the *met3* promoter has not been well studied in filamentous fungi, the *met3* promoter activity would be examined with the Beta-glucuronidase (GUS) reporter gene. The *met3* promoter was isolated from *Aspergillus nidulans* and inserted upstream of the coding region of the GUS reporter gene. The transgene expression was transformed into *A.niger*. The *met3* promoter activities under culture conditions with or without methionine are being examined. In addition, the cDNA of the polyubiquitin gene under the control of the *niaD* promoter was constructed and transferred into *A.niger*. The effects of polyubiquitin on fungal morphology are also being examined.

Additional suppressive subtractive hybridization (SSH) genes were selected for examining their effects on fungal morphology by gene deletion.

Morphology Score—*A. niger* citric acid production is analyzed by measuring the amount of citric acid made by a strain. Part of the analysis includes an examination of the morphology associated with production. To facilitate this analysis and aid in comparison between mutants, we have developed a scoring system for *A. niger* pellets. Our system is based upon the knowledge that strains that contain larger numbers of tip cells give higher production. To score a pellet, you simply draw a 10- μ m circle around the original spore. Place another 30- μ m circle around the first circle. The number of tips that appear between these two rings will be the score. The example given in Figure 2.1 shows that *A. niger* 11414 grown in normal media (Figure 2.1A) will have a score of 1. Germlings grown in citric acid production media will have numbers ranging from 3 to 7 with an average much higher than 1. To test this approach, we examined a mutant in the MAP kinase gene (Figure 2.2). The mutant makes much less citric acid and would score a 1 to 2. Data from this mutant as well as growth in normal media are consistent with this scoring system. One potential problem will be with defining what constitutes a tip. We have created green fluorescent protein (GFP) fusions to proteins known to localize to tips in fungi (Meyer et al. 2008). This GFP fusion effectively labels tips in normal media (Figure 2.3A) as well as CAP media (Figure 2.3B). We will examine multiple mutants and compare the citric acid production level to the morphology score in future work.

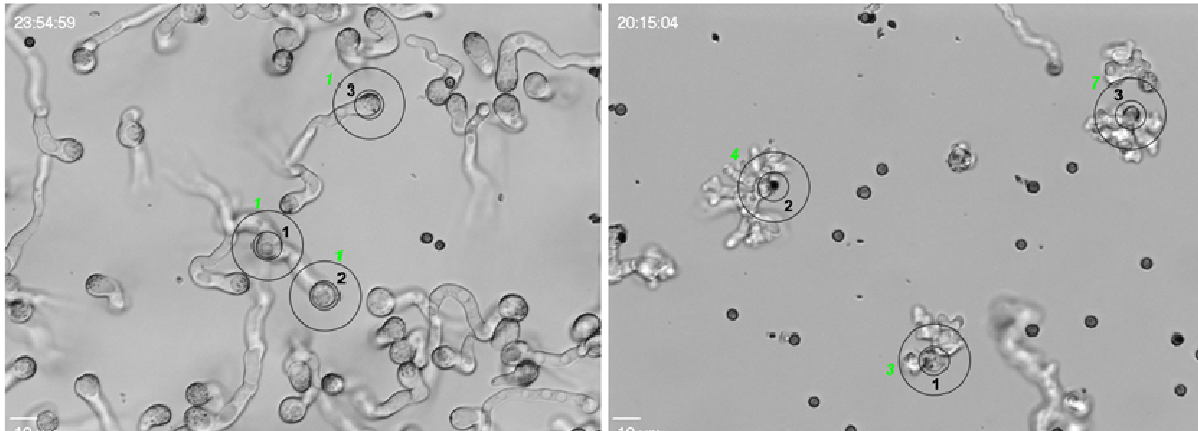


Figure 2.1. Scoring System for Fungal Morphology. The number of tips found between two concentric circles is proposed as a scoring mechanism that correlates morphology and production. In this example, germlings grown in complete media (left) are given a score of 1. Germlings grown in citric acid production media score between 3 and 4 (right). This is also consistent with citric acid production since very little is produced in complete media.

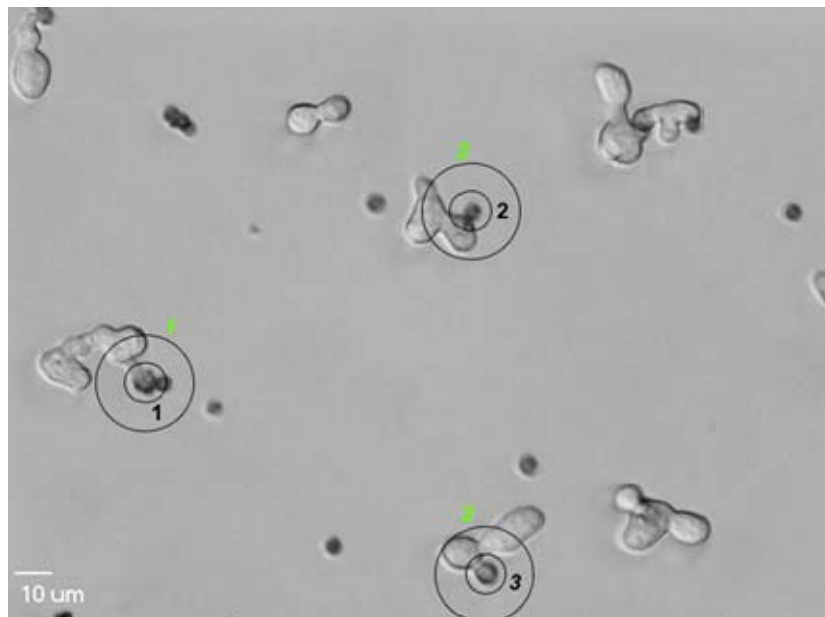


Figure 2.2. MapK1 Mutant Morphology Score. Deletion of the Mapk1 gene results in the inability to make multiple tips in citric acid production media. This leads to extremely low levels of citric acid as well as a low morphology score.

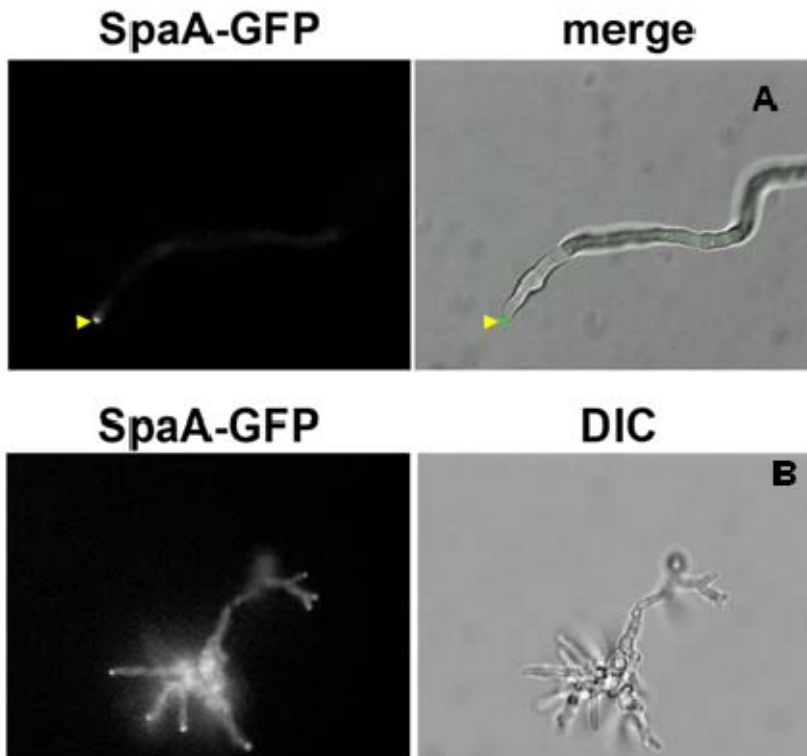


Figure 2.3. GFP as a Tool for Marking Tips. A gene fusion was made to the polarisome component SpaA. The fusion was integrated at the SpaA gene locus. This marker allows us to clearly define tips in different culture conditions, such as complete media (A) and CAP media (B).

2.3 Plans for FY10

This task is being eliminated and transitioned into a new task, **Advanced Strain Development**.

3.0 Major Subtask A.2 Fungal Genomics

3.1 Background

For decades, industrial bioprocesses, such as those that will be employed in the biorefinery, have been developed by an empirical, random approach. In other words, multiple rounds of random mutagenesis and screening have been used to improve the microbial strains involved in a time-consuming process. The advent of whole genome sequencing and global, or “shotgun,” proteomics makes targeted strain-improvement approaches an attractive alternative that may save time and money. We are using available genomics and proteomics (Subtask A.3) resources and developing additional tools to identify and/or confirm genes and regulatory elements that control fungal morphology and hyperproductivity of small metabolites (fuels and chemicals). The genome sequences of model fungi are obtained via collaboration with the U.S. Department of Energy (DOE) Joint Genome Institute (JGI). Ultimately, this subtask will provide the information and tools that are required to modify fungi predictably; in other words, metabolically engineer a fungus to produce a desired product (fuel, chemical, or enzyme) more efficiently.

We have an ongoing effort to extend our genetic analysis of *Aspergillus niger*. Candidate morphology and hyperproductivity genes are derived from analysis of the DOE JGI *A. niger* genome and the associated expressed sequence tag (EST) data. In FY07, we generated several mutants in high-level signaling pathway genes (MAP kinases), manganese homeostasis genes, and cell wall synthesis genes. In FY08, we performed genetic, functional genomics and phenotypic analyses of these and other *A. niger* genes that are potentially involved in controlling fungal morphology and organic acid production. We will continue to work with the JGI to improve fungal genome sequence resources, especially those for *A. niger*. In FY07, two close “relatives” of *A. niger* entered the sequencing queue, and their sequences are scheduled for completion in late FY08 or early FY09.

We have established a strong collaboration with the Technical University of Denmark (DTU). The DTU collaboration is important for access to additional state-of-the-art functional genomic tools. These tools include metabolic modeling software for various *Aspergillus* species and an *A. niger* Affymetrix microarray that DTU has developed. The microarray allows global monitoring of gene expression at the mRNA level (transcriptomics), which augments our global proteomic characterization of gene expression at the protein level. These two functional genome approaches provide complementary data on morphology control and hyperproductivity.

The development of efficient genetic tools is an essential part of the genomics subtask that supports the entire Fungal Biotechnology Task. Several methods for accelerated gene deletion have been applied in other organisms. These include split marker gene deletion and gene silencing using siRNA and reversible markers. We will apply these methods to our model production organisms. Another desirable capability would be a set of promoters that allow for the control of expression of target genes. In FY09, we will initiate a screen for promoters that are advantageous for production conditions.

3.2 Objectives

- Enable a high-throughput pipeline for genetic analysis of *A. niger* citric acid production (both morphology and productivity characteristics).
- Use analysis of proteomic and transcriptomic data to generate candidate genes for further characterization.
- Adapt methods used in the study of *A. niger* morphology and citric acid production for the study and subsequent engineering of *A. terreus*.

3.3 Accomplishments and Results

Overexpression—Part of our approach to understanding and improving fungal fermentation includes manipulating specific genes. This is largely done by gene deletion followed by analyzing the resulting phenotype. Another important way to analyze gene function is by overexpressing the gene. Overexpression can be achieved by promoter replacement or multiple copy integration. Promoters used in this analysis can either be constitutive or inducible. In the study of fermentation, inducible promoters that are not affected by catabolite repression are important since many of our fermentations are performed with glucose. In the past year, we have tested overexpression of genes using several combinations of promoters (Table 3.1).

Table 3.1. Fungal Expression Constructs

Promoter	Function	Reagent	Results
NiaD	Inducible	Nitrate, repressed by Ammonium	Testing
Met3	Inducible	Sulfate, repressed by Methionine	Testing
gpdA	Constitutive	None	High expression in AmA

Overexpression can be achieved with any of these promoters when integrated into a plasmid capable of being maintained through mitosis without integrating into the chromosome (Gems et al. 1991). This plasmid, referred to as AmA, contains a portion of the *A. nidulans* chromosome that allows it to be replicated and maintained during vegetative growth. We have used an AmA plasmid that contains the *pyr4* gene from *Neurospora crassa*. This marker will allow us to delete genes using hygromycin and overexpressing genes in that genetic background.

Map Kinase—Routine growth of *Aspergillus niger* includes the formation of long branching hyphae that form a web of filaments forming a mycelium. During citric acid production, filament formation is suppressed, and bulbous chains of cells aggregate into small pellets that are devoid of any extensive filamentation. The subsequent addition of manganese to a production culture causes polar growth to resume and citric acid production to cease. Previous observations indicate that these pellets contain multiple tips emanating from individual cells. In an effort to understand signaling mechanisms that control pellet formation, we deleted several MAP Kinase genes in a citric acid production strain of *A. niger* (ATCC11414). Gene deletion of an orthologue of *Magnaporthe grisea* PMK1 resulted in a strain with reduced citric acid production. This mutant displays an atypical pellet morphology with extensive apolar growth and an inability to form large pellets. Adding manganese restores filamentation; however,

this MAP kinase mutant has fewer extending hyphae than the parental strain. This is an indication that the mutant is incapable of initiating multiple sites of polar growth under these conditions.

Reversible markers—Functional genome studies depend on an efficient targeted gene manipulation system. DNA-mediated transformation requires the use of markers that allow transformants that have stably integrated the DNA of interest to be selected. A number of selectable markers have been described for the transformation of filamentous fungi, including auxotrophic mutants that are transformed with the corresponding gene and antibiotic resistance markers such as hygromycin. These routine markers are not always available for use in production strains without well developed genetic tools such as auxotrophs. Also, some fungi, such as *A. oryzae*, are resistant to certain antibiotics. A marker system must be applicable to a wide range of organisms and can be implemented without altering the productivity of the strain through mutagenesis. In past years, we have created uracil auxotrophs by manipulating the *pyrG* gene in *A. niger*. *PyrG* mutants of production strains of *A. niger*, *A. oryzae*, and *Trichoderma reesei* have been successfully produced using double-joint PCR-based homologous integration of a small deletion in the *pyrG* locus. This procedure has proven useful in making gene knockouts. This PCR approach can be adapted to any marker that has both forward and reverse selection. One such marker is the gene coding for ATP-sulfurylase. It is required for using sulfate as a source of sulfur. This enzyme also metabolizes selenate, which is analogous to sulfate and has similar chemistry. Selenate is toxic to strains that carry a functional ATP-sulfurylase gene. Therefore, mutants can be selected on media containing selenate. The resulting mutation is then no longer capable of growing on media in which sulfate is the sole source of sulfur (Figure 3.1). We have successfully created this mutation in *A. niger* 11414 by using the same approach used to create the *pyrG* auxotroph. We anticipate creating similar mutants in *A. oryzae* to increase the number of available markers in each system.

Aspergillus terreus, *A. oryzae*, *A. carbonarius*, *T. reesei*—An important part of the genomics task is to facilitate genetic manipulation in all strains of interest. We have successfully transformed and deleted genes in a variety of fungi. Table 3.2 contains a list of the status of this tool development.

***Aspergillus niger* High Throughput Gene Deletions and Analysis**—In recent years, a large-scale genome wide gene deletion project has been performed on *Neurospora crassa* (Colot et al. 2006). This approach was, in part, facilitated by the discovery of genes required for non-homologous end joining of DNA (Ninomiya et al. 2004). Using the same approach, we have adapted these tools to the citric acid-producing strain of *A. niger* 11414. A reversible gene insertion was placed into the *kusA* locus using a split marker approach used previously in *A. nidulans* (Nielsen et al. 2008). This mutation disrupts *kusA* activity and greatly increases the rate of homologous integration (Figure 3.2). However, strains lacking a functional *kusA* gene are susceptible to mutation, particularly double-stranded breaks in DNA (Meyer et al. 2007). Direct repeats of the *kusA* gene flank the *pyrG* marker in this mutation. Revertants are selected by plating on media containing FOA. We tested the mutant as well as a revertant of the mutant selected on FOA and compared these to the parental 11414 strain by exposing them to varying levels of gamma radiation. The *kusA* mutant is much more sensitive to this treatment because it is incapable of rejoining non-matching DNA strands (Figure 3.3). The revertant was no longer as sensitive to the treatment, indicating the restoration of the *kusA* function in these strains.

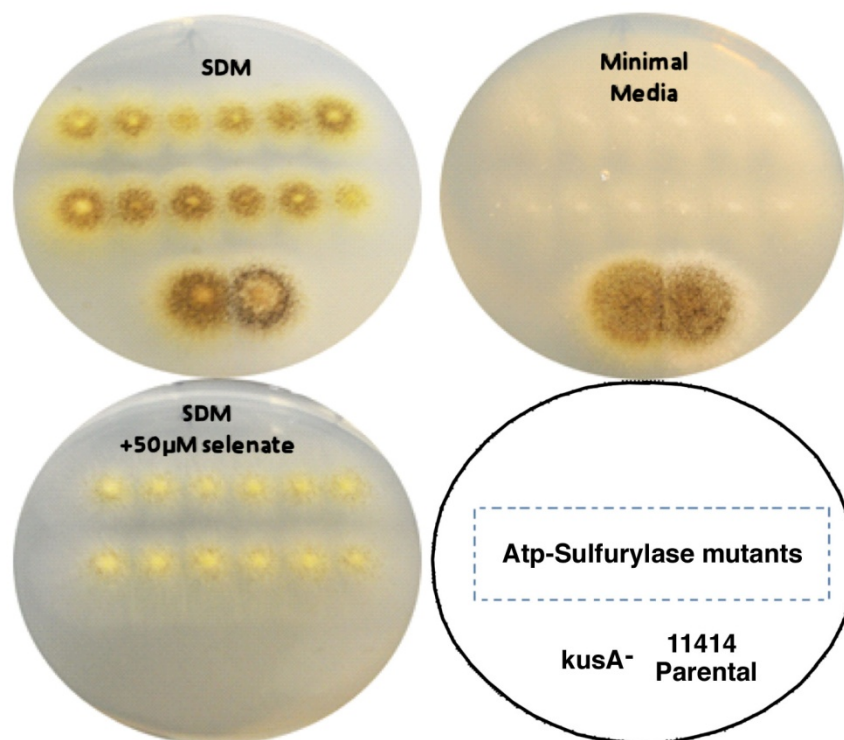


Figure 3.1. Mutation of ATP Sulfurylase in *A. Niger*. The ATP sulfurylase gene can be used as a reversible genetic marker. Cells lacking this gene are insensitive to 50 μ M selenate (bottom left) but require the addition of methionine and cannot grow on minimal media containing only sulfate as a source of sulfur (top left) (sulfate depleted medium [SDM]).

Table 3.2. Genetic Markers Available for Gene Manipulation in Relevant Strains

Species	Transformation	Markers	Deletions
<i>A. terreus</i> ATCC 32359	Protoplast, KCl	Hygromycin, Bleomycin	5 genes
<i>A. oryzae</i> NRRL697	Protoplast, Ammonium Sulfate	<i>pyrG</i>	4 genes
<i>Trichoderma reesei</i> QM6A	Protoplast, MgSO ₄	<i>pyrG</i> , Hygromycin	3 genes
<i>A. carbonarius</i>	Protoplasts, MgSO ₄	Hygromycin	Hyg integration, 0 deletions
<i>A. niger</i> ATCC11414	P Protoplast, Ammonium Sulfate	Hygromycin, Bleomycin, <i>pyrG</i> , Sc	40+ genes deleted

Using the *KusA* mutant, we have initiated a high throughput deletion protocol to analyze citric acid production. A modified version of the Primer3 software for automatically picking primers for all genes within a genome was obtained from Dr. Hildur Colot at Dartmouth University. The software was adapted to process genomes and gene-feature annotation files downloaded from the Broad Institute's collection of *Aspergillus* genomes. Out of 11200 *A. niger* genes, the program was capable of automatically picking primers for 11030 genes. Primers for 32 of these genes were synthesized and successfully used to amplify the targeted genes.

One advantage of using the *kusA* mutant is that it greatly reduces the effort needed for screening the deletions. The homologous transformation rate is close to 100%. This allows us to reverse the usual order of this type of analysis. We can pick transformants and screen for phenotype first. Transformants that display changes in morphology or citric acid production can then be screened to verify proper integration and gene deletion. Figure 3.4 demonstrates a plate assay for growth in citric acid production media. Six transformants of the *A. niger* 11414 *kusA*⁻ strains were picked for each gene. Spores were replica plated using a pin replicator. This analysis shows that the manganese transporter, *smfA*, forms much tighter colonies on this medium and is likely required for Mn uptake in these conditions. This type of plate screen will help accelerate genetic analysis of *A. niger*. We plan to delete large classes of genes, including all genes thought to play a role in MAP Kinase signaling as well as genes involved in reactive oxygen species generation and mitigation.

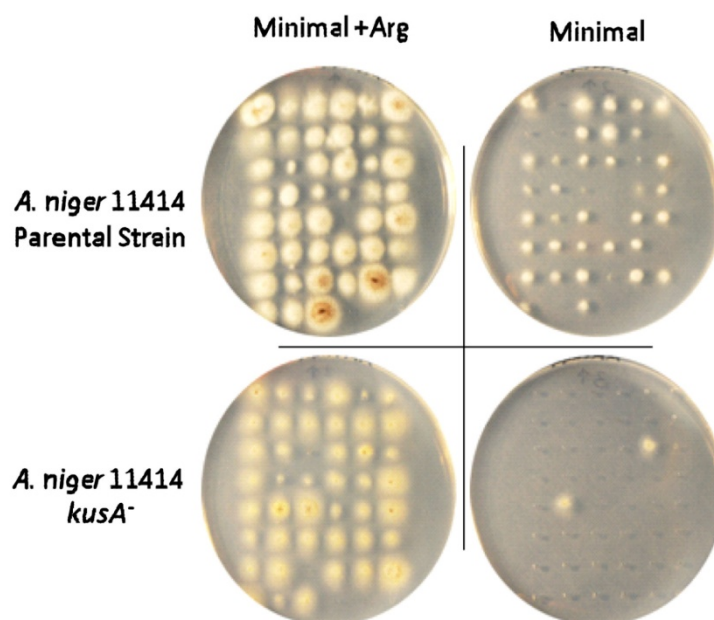


Figure 3.2. Improved Homologous Recombination in the *kusA* Mutant. Colonies grown from wildtype and *kusA*⁻ spores collected from individual *ArgB* knockout transformants. Colonies in which homologous recombination occurred grew on media containing arginine, but did not grow on media lacking arginine. Using the *argB* gene as a test, we have seen an increase in homologous recombination from 20% in the parental strain to 95% in the *kusA*⁻ strain.

Joint Genome Institute Project Leads—Jon Magnuson: *Dunaliella salina* genome, Columbia River periphytan population census and Scott Baker: *Aspergillus niger*, *Trichoderma atroviride*, *Piromyces*, *Orpinomyces*, *Aspergillus aculeatus* and *Aspergillus carbonarius* genomes, *Aspergillus terreus* ESTs.

3.4 Plans for FY2010

The DOE has made and continues to make a large investment in fungal genome sequencing at the Joint Genome Institute. The goal of the Fungal Genomics Task is to use genomic, proteomic, and transcriptomic experimental data to enable rapid and high-throughput methods for discovery and

functional characterization of genes that are potentially involved in fungal morphology control and organic acid and enzyme hyperproductivity. Using *Aspergillus niger*, we will apply successful strategies from this model system to other fungi, including *A. terreus*. The activity in this task not only draws data from the other tasks; it also directly supports them by generating and analyzing various mutant strains for use in proteomic, morphology, and fermentation experiments. Planned accomplishments for the year include:

- Promoters ranked according to their characteristics
- Phenotype analysis of six signaling/transcription factor/reactive oxygen species (ROS) genes in *A. niger* and/or *A. terreus*
- *Trichoderma reesei* cellulase improved strains sequenced in collaboration with DOE Joint Genome Institute
- Construction of six signaling/transcription factor/ROS genes in *A. niger* and/or *A. terreus*
- Make KU mutants in *A. terreus* and *A. oryzae*.

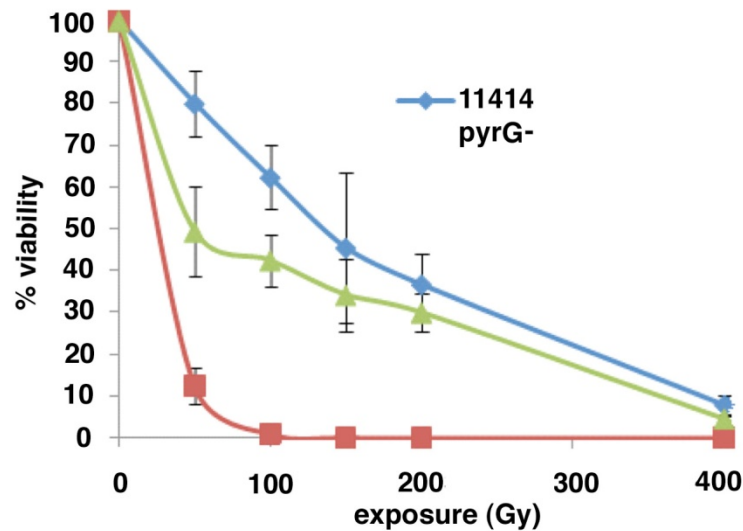


Figure 3.3. The Percent Viability of Wildtype, *kusA*⁻, and *kusA*⁺ Revertant Spores Exposed to Gamma Radiation. The percent viability of the *kusA*⁺ revertant is very similar to that of the wildtype and significantly higher than that of *kusA*⁻, demonstrating that the *kusA*⁺ revertant has restored capability to repair DNA.

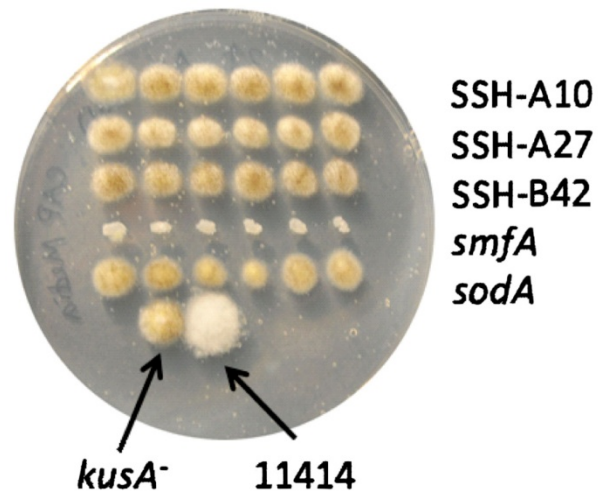


Figure 3.4. Phenotype Screen of Five Mutants (six colonies each) on CAP Media. The *Smf* mutant displays a unique phenotype in all six colonies, illustrating the high rate of homologous recombination in the *kusA*⁻ strain.

4.0 Major Subtask A.3 Fungal Proteomics

4.1 Background

Proteomics has been defined as the study of the “protein complement expressed by a genome” (Wilkins et al. 1996). With current technology, a single MS analysis in which peptides are eluted into the instrument directly after separation by LC can identify thousands of parent proteins. Several methodologies have been described for global relative protein quantitation between two separate samples using these techniques (Wilkins et al. 1996; Conrads et al. 2000; Gao et al. 2003; Gygi et al. 1999). We have applied this technology to the study of morphology control and hyperproductivity in filamentous fungi. We expect that the discovery of proteins whose abundances differ in the pelleted and filamentous growth states of *A. niger* will identify proteins involved in the control of cellular processes related to morphology determination.

Our goal is to have a rigorous global proteomics procedure developed and demonstrated that proceeds from experimental design all the way through data interpretation. Relative quantitation between the two growth conditions is performed using mixed-effects statistical modeling (described in detail in Daly et al. 2008). One peptide may be more easily detected and quantified by the mass spectrometer than another peptide of equal molarity due to the physical properties of the peptide (number of sites available for protonation, hydrophobicity, etc.). In other words, two peptides resulting from trypsin digestion of one protein may not be detected with equal sensitivity, which causes problems when combining abundance measurements from different peptides of the same parent protein. However, the relative response of the instrument to one peptide compared to another is independent of other factors in an experiment, such as dilution. This relationship allows for the relative peptide response to be estimated and subsequently corrected, which provides more precise estimates of protein abundances by pooling information across peptides.

4.2 Accomplishments and Results

Our proteome analysis of *A. niger* under filamentous and pelleted growth conditions included nine biological replicates. Each of the two samples for a biological replicate was split into three separate tubes for samples processing. All samples had two LC/MS injections, yielding a total of 108 data sets. Overall, 729 proteins were observed sufficiently to be modeled out of a total of 1735 proteins identified. As is often the case with “shotgun” proteome analysis, a significant number of proteins were observed only once during the analysis (500). Of the proteins modeled, 353 had p-values calculated to be less than 0.05. Proteins modeled had relative abundances that ranged from 0.3- to 4.2-fold differences between the two growth states.

Of particular interest are those proteins that were indicated to be highly differentially expressed between the two conditions. The 19 proteins identified in the analysis that were calculated to have the highest relative abundance in filamentous cells are presented in Table 4.1. The range of relative abundances in the corrected Table 4.1 is 1.5 to 4.4 fold. Similarly, modeling indicated that 13 proteins identified to be approximately half as abundant in filamentous relative to pelleted cells had calculated p-values less than 0.05 (Table 4.2). The results present some intriguing protein targets for additional study. Ribosomal protein L34, which was identified as more abundant in pelleted cells, has been

identified as an inhibitor of cyclin-dependent kinases (Moorthamer and Chaudhuri 1999). Would over expression of this gene affect cell cycle? Ornithine decarboxylase is the initial step in the polyamine pathway. Polyamines are implicated in cell growth in differentiation in several eukaryotes, which makes it another attractive target for genetic manipulation. We have spent most of our effort on identifying proteins with convincing identifications from blast analysis whose expression could be verified by enzyme or Western analysis. To that end, we focused on protein ID 47229 (phytase), 214686 (oxalate decarboxylase), and 213198 (peptidyl-prolyl cis-trans isomerase B) (Table 4.1).

Table 4.1. Proteins Higher in Abundance in the Filamentous vs. Pelleted Growth State

JGI ID	Blast ID	Score	E-Value	Notes
206270	Srp68, <i>Canis familiaris</i> .	377	4e-35	Subunit of signal recognition particle, targets secretory proteins to ER
47229	PhyB, <i>Aspergillus awamori</i>	2274	0	3-Phytase B
210783	Pmp20, <i>Aspergillus fumigatus</i>	639	2e-66	Peroxiredoxin pmp20
37155	Uncharacterized	253	2e-21	From Acanthamoeba polyphaga mimivirus
214686	OxdC, <i>Bacillus subtilis</i>	1082	1e-117	Oxalate decarboxylase
207705	Rpn9, <i>Schizosaccharomyces pombe</i>	847	6e-90	26S proteasome regulatory subunit
184329	FaeA, <i>Aspergillus awamori</i>	253	3e-21	Feruloyl esterase A
199424	None			
191172	Bgl2, <i>S. pombe</i>	246	2e-20	Glucan 1,3-beta-glucosidase
213198	PpiB, <i>Aspergillus niger</i>	1024	1e-111	Peptidyl-prolyl cis-trans isomerase B
201930	Rpl24, <i>Neurospora crassa</i>	379	3e-35	60 S ribosomal protein L24
54717	None			
56985	Tcb1, <i>Saccharomyces cerevisiae</i>	1384	1e-151	Tricalbin-1
41962	Smd2, <i>S. pombe</i>	342	3e-32	Small nuclear ribonucleoprotein Sm D2
130857	Sdh1, <i>S. pombe</i>	2014	0	Probable succinate dehydrogenase subunit
207660	FksA, <i>A. niger</i>	9361	0	1,3-beta glucan synthase subunit
48843	SudA, <i>Emericella nidulans</i>	5239	0	Chromosome segregation protein sudA
209528	Rnc1, <i>S. pombe</i>	733	1e-76	RNA-binding protein rnc1
210479	Mcm7, <i>S. pombe</i>	2218	0	DNA replication licensing factor mcm7

Table 4.2. Proteins Higher in Abundance in the Pelleted vs. Filamentous Growth State

JGI ID	Blast ID	Score	E-Value	Notes
209511	Rpl34, <i>Saccharomyces cerevisiae</i>	410	4e-40	60S ribosomal protein L34b
54942	Ak, <i>S. cerevisiae</i>	958	1e-102	Aspartokinase
53577	Uncharacterized, <i>Schizosaccharomyces pombe</i>	610	2e-62	
128537	Aspf7, <i>S.pombe</i>	264	4e-23	Allergen
208611	Uncharacterized, <i>S. pombe</i>	218	e-17	
212190	Imb3, <i>S. pombe</i>	2319	0	Importin subunit beta 3
190790	Ecm33, <i>Aspergillus fumigatus</i>	1024	e-110	Glycosylphosphatidylinositol-anchored protein involved in cell wall biosynthesis
212716	Gel4, <i>A. fumigatus</i>	1265	e-138	1,3-beta-glucanosyltransferase gel4
212102	Rpl27, <i>S. cerevisiae</i>	505	4e-51	60S ribosomal protein L27a
212069	Uncharacterized, <i>S. pombe</i>	160	3e-10	HTH APSES-type DNA-binding domain containing protein
200566	Egd2, <i>Aspergillus niger</i>	598	2e-61	Nascent polypeptide associated complex subunit alpha
46787	Tma29, <i>S. cerevisiae</i>	689	8e-72	Uncharacterized oxidoreductase
127054	Isu2, <i>S. cerevisiae</i>	457	6e-45	Iron sulfur cluster assembly protein 2

We initially attempted to assay phytase with an assay kit. The kit is a coupled reaction that releases a fluorescent reaction product for detecting phytase activity. *A. niger* was grown in CAP media with and without manganese. Cell extracts were prepared by freeze grinding fungal biomass and then subsequently solubilizing the material in phytase reaction buffer. Spent media samples were prepared for assay from the two conditions by filtering through a 2-micron membrane. Phytase from wheat was used as a positive control. As shown in Figure 4.1, activity was detected in both cell extracts with slightly higher activity in pelleted cells as compared to filamentous. However qualitatively when the spent media extracts are compared, there is significant phytase activity detected under filamentous conditions over the background given by CAP media. The combined intracellular and extracellular phytase activities support the data from the proteomics work which, indicated that phytase is more abundant in *A. niger* grown under filamentous conditions. Due to the interference by CAP media in the assay, we have begun phytase assays with the method described in Piddington et al. (1993) to obtain quantitative phytase activities.

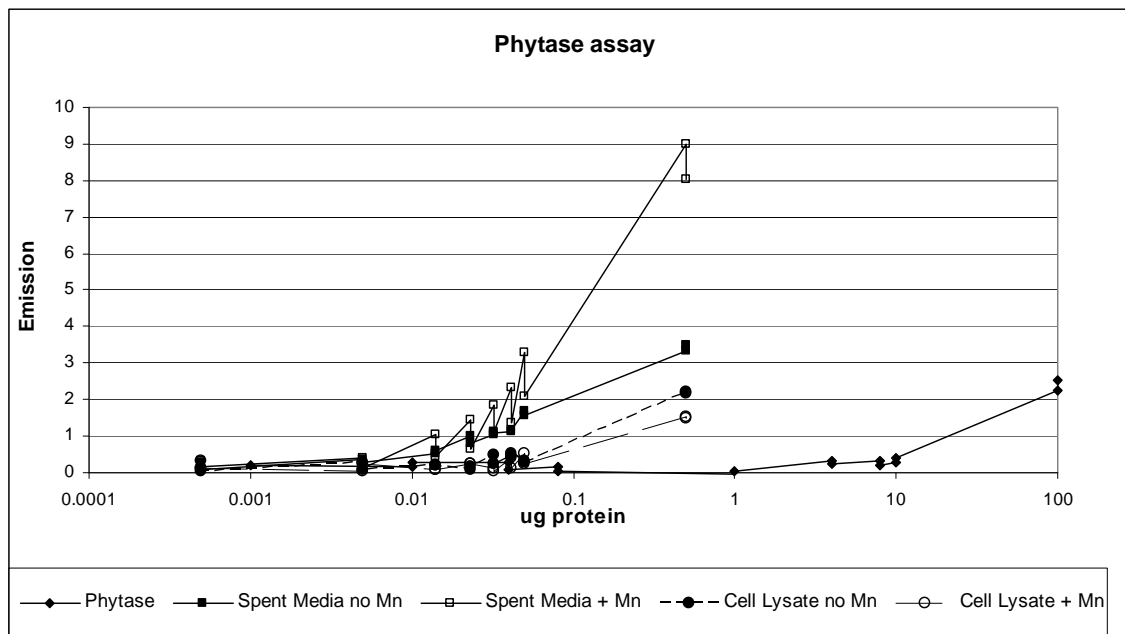


Figure 4.1. Phytase Assays on Phytase from Wheat and Cell Lysates and Spent Media from *A. niger* Grown Under Filamentous (+ Mn) and Pelleted Conditions (no Mn)

Oxalate decarboxylase activity of cellular lysates was performed as described in Bergmeyer et al. (1985, pp. 126-327). Again, *A. niger* was grown in CAP media both with and without manganese with extracts being prepared by freeze grinding fungal biomass. The cell extract was solubilized in 100 mM phosphate buffer, pH 5. Extracts from filamentous cell lysates had an average oxalate decarboxylase activity of 3.1 units/ml (± 0.2), while no activity could be detected in extracts of pelleted cells. This corroborates the proteomics data, which indicated that oxalate decarboxylase is higher expressed in *A. niger* under filamentous growth conditions.

JGI gene model 213198, identified as peptidyl-prolyl cis-trans isomerase B (PPIB) by blast analysis, has significant homology to cyclophilin B (Figure 4.2). An antibody to cyclophilin B was available commercially, and it was used to perform Western analysis on cell lysates from *A. niger* grown under filamentous and pelleted conditions (four biological replicates). Results are shown in Figure 4.3(A) and Figure 4.3(B). PPIB is predicted to have a molecular weight of 23 kD. As seen in Figure 4.3(A), there appears to be some cross reactivity between the anti-cyclophilin B antibody and some proteins around 30 kD and 40 kD. Focusing in on the region around 20 kD (Figure 4.3(B)), we observe three protein bands (labeled A, B, and C) that might be PPIB or its degradation products. Both protein bands B and C and also the summed intensity of all three bands were determined by densitometry to be greater under filamentous conditions (with manganese) than pelleted. These results support the proteomic data analysis. However, protein band A is not consistent with the proteomic data and in addition is not consistent across replicates.

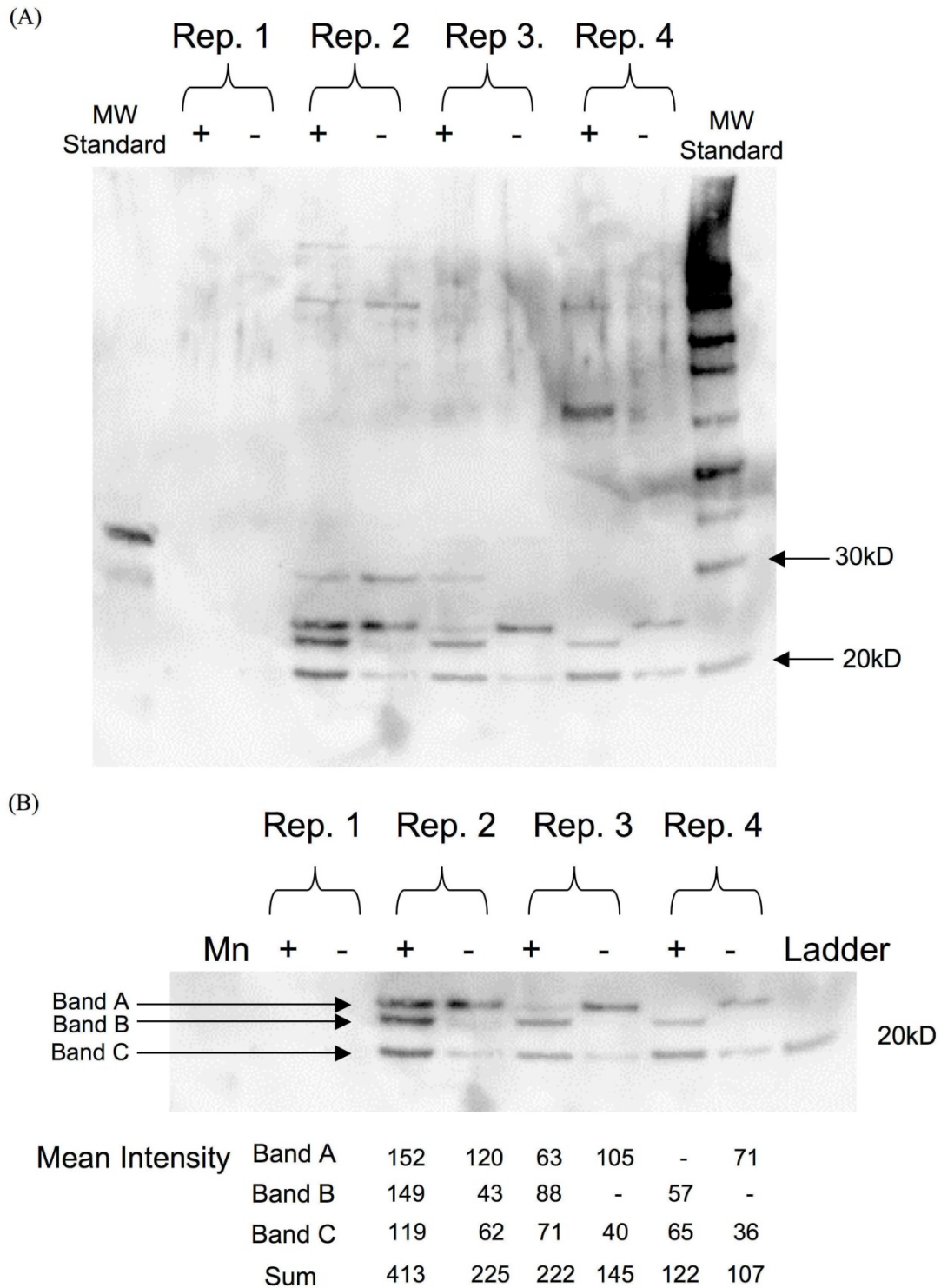


Figure 4.3. Anti-Cyclophilin Western Analysis to Identify Expression of JGI Gene Model 213198 from Cell Extracts of Filamentous (+ Mn) and Pelleted (-Mn) from *A. niger* Cultures

We ran a gel in parallel with a Western analysis and excised a 5-mm band from each sample lane centered about the 20-kD line and performed in-gel tryptic digestion for LC/MS analysis. However, an *A. niger* gene deletion strain of PPIB for additional Western analysis may be required to definitively identify which band is PPIB.

Proteome analysis was also performed on affinity-purified samples produced under subtask A.1. A histidine-tagged version of the ubiquitin gene was transformed into *A. niger*, and proteins that were bound to ubiquitin were isolated from the cell lysate. Three replicates were performed for *A. niger* grown in CAP media with and without manganese added. Elution off the nickel column was done step-wise by pH, resulting in three separate eluates per sample. Triplicate LC/MS injections were performed for a total of 54 LC/MS datasets. An overview of the analysis is presented in Table 4.3. A complete report is presented in Appendix A (attached as a word document). The analysis revealed that ubiquitin-associated proteins under the two conditions are fairly similar; the 15 proteins that were most often observed in the analysis are identical under either filamentous or pelleted growth conditions. Several 60S ribosomal proteins, an RNA helicase, actin, citrate synthase, and fructose biphosphate aldolase were among the proteins identified most frequently. Only two proteins (each being observed three times) were identified as associated with ubiquitin and only when isolated from cells grown in CAP media. This was without added manganese (gene model numbers 124156 [transhydrogenase by blast] and 190014 [phosphate reductase involved in proline biosynthesis]). There were more than a dozen proteins (again with two or three observations) that were only observed as ubiquitin associated when isolated from cells grown in CAP media with manganese, including oxalate decarboxylase, formate dehydrogenase, and a protein required for nuclear migration within hyphae (nudE). A cell morphogenesis protein (gene model 38101) and several kinases identified in the analysis (gene model numbers 52248, 207707, 36874, 214022, and 35734) are attractive targets for additional investigations.

Table 4.3. A Summary of Identifications from Affinity-Purified Ubiquitin

Sample Description	Number of Datasets	Total Number of Peptides Observed	Number of Unique Peptides Observed	Number of Unique Proteins Observed
No Mn, pH 4.5	9	389	81	42
No Mn, pH 5.0	9	1547	225	119
No Mn, pH 5.5	9	7483	1171	534
Mn, pH 4.5	9	373	74	37
Mn, pH 5.0	9	876	171	85
Mn, pH 5.5	9	8874	1273	574

Following are two related Laboratory Directed Research and Development (LDRD) projects:

- A multidisciplinary approach to engineer xylose and arabinose utilization for ethanol production by *Saccharomyces cerevisiae*.
- Identification of proteomic profiles and biomarkers in complex microbial systems absent of genomic sequence data.

4.3 Plans for FY2010

We plan to:

- Provide a report on the global proteome analysis of the *A. niger* genetically modified strain to the parental *A. niger* strain for each strain
- Perform global proteomics on two genetically modified *A. niger* strains.

5.0 Major Subtask A.4a Fungal Hyperproductivity

5.1 Background

The objectives of Subtask A.4a are to:

- Discover genes that are critical for various hyperproductive processes in fungi
- Develop tools and techniques with a model fungal producer of small metabolites and enzymes that can be widely applied to other hyperproductive fungal systems.

The objectives of this task are to support the overall goals of the project by providing targets for genetic engineering of fungi that will ultimately accelerate the development of novel enzyme or small molecule processes. They will also lead to improvements in current processes, including the utilization of different complex carbon feedstocks. This task is highly integrated with the others. It will rely in part on the tools and processes from Task A.2 to discover target proteins and their genes and manipulate the target organism, which will require the tools developed through Tasks A.1 and A.2. The study of the organism in authentic fermentation conditions with different nutrients, such as complex carbon sources, will use the tools from Task A.4b.

The model organism and process selected for study is *A. terreus* and its production of the small metabolite itaconic acid and biomass hydrolyzing enzymes. This fungus has a genome sequence available from the Broad Institute and has been the subject of a variety of past studies. The literature, however, is far less extensive than for *A. niger*. The morphology of the fungus in submerged fermentations is well behaved, though it does not exhibit the ideal pelleted morphology, so there is room for improvement. With the use of *A. terreus* for the “Hyperproductivity” and “Biomass to Products” tasks and *A. oryzae* for the “Fungal Ethanol” task, all of our tasks now use *Aspergillus* spp. as model organisms. This should facilitate the transfer of knowledge and genetic traits from one task and organism to another, e.g., morphology control genes from *A. niger* into *A. terreus*. The large number of functional genomics and modeling tools available for the Aspergilli also make these attractive model organisms.

The hyperproductivity of fuels, chemicals, and enzymes in fungi is a phenotype that is almost certainly associated with multiple genes. In addition to enzymes of the primary metabolic pathways leading to the production of small metabolites (fuels and chemicals) or amino acids for enzymes, other proteins likely to be important in hyperproductivity include substrate (sugar) and product transporters (Magnuson and Lasure 2004). Potentially these could be mitochondrial or plasma membrane or both types of transporters for key organic acids. Putative sugar and organic acid transporters in the *A. terreus* genome are being identified *in silico* using the genome sequence data. However, the functions of most transporters, even within a known protein family, cannot be verified based on sequence information alone. Also, we do not know all of the genes associated with increased or decreased organic acid production in fungi; therefore, discovery-based approaches will be needed to supplement rational biochemical and genomic pathway analyses.

In FY08, we prepared RNA samples from three different stages in the itaconic acid production process of *A. terreus* (before production begins, onset of production, and maximum production phase) and submitted them to JGI for cDNA preparation and EST sequencing.

5.2 Accomplishments and Results

In FY09, we have made considerable progress in understanding the production of itaconic acid at the gene and transcript level and thus identifying potential genes for analysis with regard to their effect on this process. This progress was facilitated by the receipt of the *A. terreus* EST data from JGI. These data consisted of sequences for the cDNA derived from the mRNA for three different stages in itaconic acid production by *A. terreus* grown on a medium containing 10% glucose. The stages were as follows: 1) “pre,” before itaconic acid production begins, 2) “onset,” at the beginning of itaconic acid production (correlates with phosphate depletion), and 3) “production,” early in the phase of maximum itaconic acid production rate (see Figure 5.1).

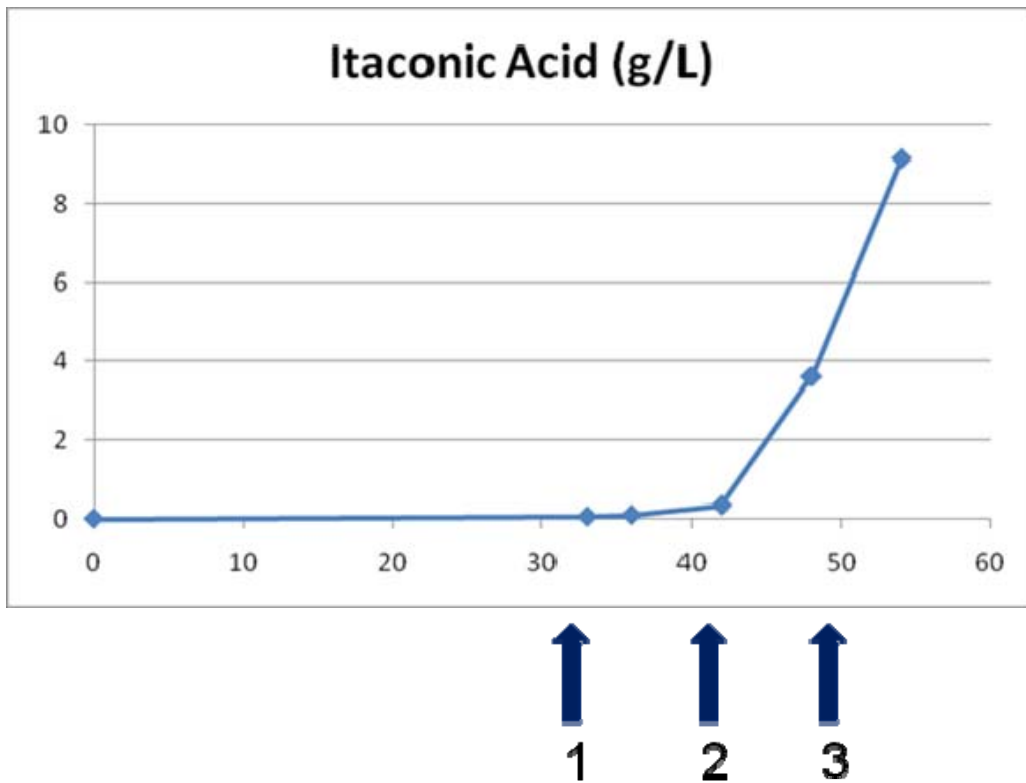


Figure 5.1. 20-L Fermentation of Glucose to Itaconic Acid by *Aspergillus terreus*. Samples were taken at the times indicated (arrows).

It was known from the literature that the enzyme responsible for itaconic acid production, *cis*-aconitate decarboxylase, is induced by itaconic acid production conditions. Analyses of the data quickly revealed a transcript that appeared with high frequency (79 ESTs) in the *onset* phase that we identified as the *cis*-aconitate decarboxylase based on 100% identity to a gene that had recently been entered into GenBank. This transcript did not appear in the other two stages, indicating that it is turned on strongly at the *onset* of itaconic acid production and then quickly degraded, though the enzyme obviously persists throughout the *production* phase. The immediate identification of the *cad* gene eliminated the need for an activity we had planned for this year, which was a general search of the EST data for all decarboxylase genes.

Another gene that was strongly transcribed in the *onset* phase was identified as having homology to a “putative mitochondrial transport protein” (YFR045W) in *S. cerevisiae*. We located these two genes on the Broad Institute’s *A. terreus* genome browser, which showed that they were in a cluster immediately adjacent to the lovastatin biosynthesis cluster (see Figure 5.2). A transcription factor is located upstream of the YFR045W homolog and the *cad* gene, while a major facilitator superfamily (MFS) transporter is located immediately downstream of the *cad* gene. These four genes quickly entered our list of gene candidates for deletion to determine their effect on itaconic acid production. The transcription factor is especially exciting since this could control the putative “itaconic acid production cluster.”

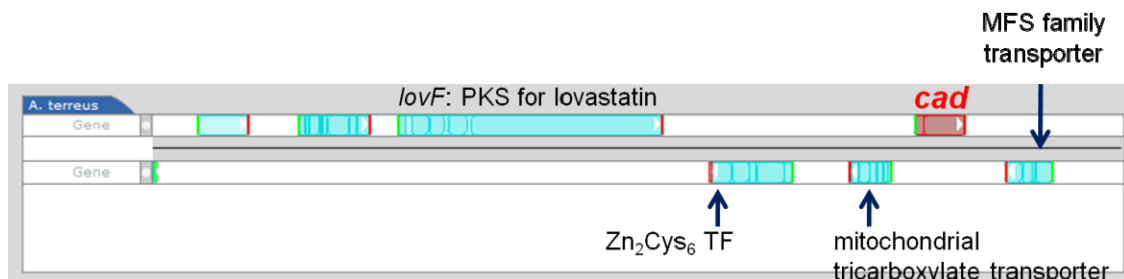


Figure 5.2. Snapshot of the *Aspergillus terreus* Chromosome Region Containing the Lovastatin and Itaconic Acid Gene Clusters

At the close of the last fiscal year continuing through April of 2009, we had been unable to re-establish the *A. terreus* transformation procedure that was lost upon the move from the main PNNL campus to Bioproducts, Sciences, and Engineering Laboratory (BSEL). At the Fungal Genetics Conference in Marc, Dr. Deng had discussions with other investigators who had previously transformed *A. terreus*. This led to some fresh approaches that ultimately proved successful in her hands. With the transformation system working again, we have proceeded to knock out four additional genes (through Aug 2009). The genes knocked out are as follows: *phyA* (phytase, deleted last year), *creA* (a transcription factor involved in carbon catabolite repression of many genes, including cellulases), *cad*, the mitochondrial transporter gene, and the transcription factor. Initial testing of these knockout mutants on itaconic acid production media in shake flasks will be done in the remainder of the fiscal year.

5.3 Plans for FY2010

- Continue to evaluate the EST data to generate leads for analysis by deletion and/or over-expression. Focus on transcription factors and kinases that regulate many genes or a pathway.
- Generate additional knockouts in *A. terreus* based on the evaluation of the EST data.
- Continue evaluation of current and new knockouts for itaconic acid production vs. wild type *A. terreus* in shake flasks and fermentors when appropriate.
- Express the *A. terreus* *cis*-aconitate decarboxylase gene in *A. niger* and evaluate the performance of this strain in shake flasks under citric acid production conditions.

6.0 Major Subtask A.4b Consolidated Bioprocesses

6.1 Background

This task is focused on the understanding and development of single vessel bioprocesses for the conversion of complex biomass to fuels, organic acids, and enzymes. Task A.4b is concerned with developing, implementing, and optimizing fermentation processes and analytical techniques to examine the fungi developed in the other tasks with regard to morphology, productivity, and utilization of complex biomass in submerged fermentations. Specifically, this effort will investigate the conversion of complex biomass to products in fermentations using *Aspergillus* spp.

6.1.1 Specific Objectives

- Develop and implement techniques for studying fungal bioprocesses for the conversion of simple and lignocellulosic feedstocks to fuels, chemicals, and enzymes.
- Develop *A. terreus* and itaconic acid production as a model complex biomass to organic acid process.
- Investigate *Trichoderma reesei* as a model enzyme over-production organism using complex biomass.

Simplified biomass to products approaches have been called “simultaneous saccharification and fermentation” (SSF), “consolidated bioprocessing,” and “direct microbial conversion.” All of these terms describe a single vessel fermentation in which an organism grows on the complex biomass, produces the enzymes to hydrolyze the biomass to sugars, and uses the sugars to make products. The concept is appealing in that it requires fewer handling steps and less capital equipment, therefore making it potentially more economical. It is a simple concept but difficult to execute. It requires organisms capable of producing the correct suite of enzymes to degrade a particular lignocellulosic feedstock at sufficient quantities to perform the saccharification in a timely manner and preferably simultaneously (or sequentially) convert all of the hexose and pentose sugars to fuels, chemicals, or other products. The fungal kingdom is an ideal realm from which to recruit such organisms.

Given the challenges facing the implementation of simplified bioprocesses, it is important when examining particular aspects of a bioprocess that the entire process be considered as the framework for study. The overall bioprocess variables are included in the following steps: complex biomass pretreatment, fungal organism preparation, fungal bioprocessing, and product recovery. In this program, we are focused on fungal bioprocessing, but the other key variables are still integral to the thought progression in studying the complete biomass to products process.

6.2 Accomplishments and Results

We have performed replicate fermentations with *A. terreus* using glucose or xylose as the substrates to produce itaconic acid, and the results verify that fermentations with both carbon sources reach relatively high titers and are reproducible, although the rate is lower with xylose versus glucose. Itaconic acid was produced using enzymatically hydrolyzed ground corn (i.e., starch to glucose). Baseline runs with wet distillers grains (WDG) as the sole carbon source were performed. This material has little

residual starch, just cellulose, arabinoxylan, and protein. As expected, no itaconic acid was detected, but the baseline case was important to establish. Detecting small amounts of sugars (glucose, xylose, and arabinose) that indicated that the structural polysaccharides were being degraded suggests that the fungus can use the biomass, but not produce sufficient sugar to support itaconic acid production. These runs were not supplemented with free sugars nor were any pre-treatments performed. We learned the challenges to be expected when handling high concentrations of particulate biomass. With the recovery of the transformation method for *A. terreus*, we were able to generate a *creA* deletion strain, which will be evaluated next FY.

Baseline runs of *Trichoderma reesei* QM6a (wild type) and RutC30 (over-production mutant) using glucose or cellulose with a small amount of glucose as carbon sources were performed. Key indicator biomass hydrolyzing enzyme activities were assayed to examine the variations between the strains. An example run is shown in Figure 6.1. A recent paper comparing the two strains of *T. reesei* indicates the multiple genetic differences between the strains. The numerous changes in *T. reesei* RutC30 are not surprising since this strain was derived in the traditional manner using multiple rounds of mutagenesis. As a start towards developing a genetically well defined enzyme production strain, we have knocked out one of the key genes, *creA*, previously identified as being critical to over-production of glycoside hydrolases in RutC30.

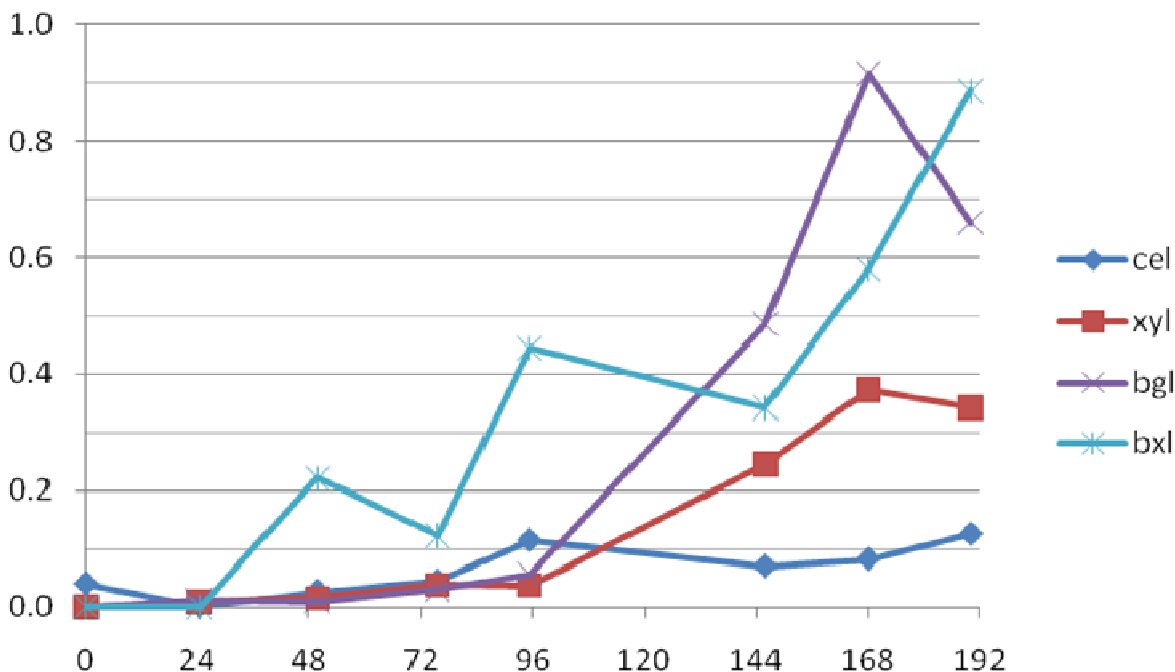


Figure 6.1. Enzyme activities in *Trichoderma reesei* QM6a Grown on Cellulose

Trichoderma reesei was grown in 10 L of chemically defined medium containing 2% cellulose and 1% glucose at pH 5.5, 30°C. Aliquots of the cleared media were assayed for cellulase (cel, endoglucanase), xylanase (xyl), β -glucosidase (bgl), and β -xylosidase (bxl). The x-axis shows time in hours after inoculation of the media with spores of *T. reesei* (5×10^5 per mL) while the y-axis shows absorbance units (relative enzyme activity). The dissolved oxygen (DO) concentration declined rapidly

and then rose as glucose was depleted. DO began to decline again at 48 hours, and enzyme activities were observed to rise at this time point or later as the fungus was challenged with growing on cellulose.

6.3 Plans for FY2010

- Examine the *creA* deletion strain of *A. terreus* on complex biomass, with or without pre-treatment, in shake flasks and fermentors. Analyses will include itaconic acid production and enzyme activities.
- Examine the *creA* deletion strain of *T. reesei* on complex biomass, with or without pre-treatment, in shake flasks and fermentors. Analyses will focus on enzyme activities. The wild-type strain QM6a will serve as the control.

7.0 Major Subtask A.5 Alternative Fungal Ethanologen Characterization and Metabolic Model Analysis

7.1 Background

Like yeast, filamentous fungi possess the ability to produce ethanol when grown in low oxygen/ anaerobic culture conditions. However, in contrast to yeast, filamentous fungi are able to degrade lignocellulosic biomass, including cellulose and hemicellulose, as well as efficiently use xylose and other pentose sugars. Thus, filamentous fungi represent a direct path from biomass to ethanol, minimizing expensive pretreatment processes.

Despite their positive characteristics and perhaps due to their inherent biological complexity compared with yeast or bacteria, filamentous fungi have only been explored as ethanol production organisms in a limited way. This subtask focuses on the characterization and optimization of filamentous fungal ethanol production from both simple sugars and directly from lignocellulosic biomass. The primary objectives of this research are to gain a fundamental understanding of filamentous fungal ethanol production processes and to discover and evaluate the potential for fungal ethanol production. While the development of an industrial strain is not the objective of this subtask, it is expected that the ethanologen discovery and improvement efforts of this research will lead to 1) a strain that clearly demonstrates that there is industrial potential for filamentous fungal ethanol production and 2) tools that industry can apply to the development of efficacious industrial filamentous fungal ethanol processes.

For FY09, we planned to:

- Validate select metabolic models and apply models to *Aspergillus oryzae* ethanol fermentations and begin Constraint-Based Reconstruction and Analysis (COBRA) analysis of *A. oryzae*.
- Develop a high-throughput screening method to rapidly identify highly productive filamentous fungal ethanologens with the deliverable being a test or tests for screening fungi for ethanol production adaptable to 96-well format or a similar medium throughput format.
- Identify individual genes that improve ethanol production in filamentous fungi using genome-wide gene knock-out and overexpression methods and apply them to the model strain.
- Order materials for genetic analysis of candidate ethanol production genes.

Our accomplishments and results for FY09 and our plans for FY10 are reported in the sections that follow.

7.2 Accomplishments and Results

7.2.1 Metabolic Modeling

In FY09, we developed capabilities to perform flux balance analysis (FBA) (Rocha et al. 2008) to computationally simulate the fluxes of substrates and metabolites through all known chemical reaction and transport pathways that comprise the metabolic network of *A. oryzae*. FBA was successfully applied to a genome-scale stoichiometric network model for *A. oryzae* to predict expected changes in ethanol

output as a function of decreasing levels of available oxygen. The WV1314 model used in this work had been published in early 2009 by our collaborators at Chalmers University, but in a proprietary format compatible only with their unpublished, in-house software (Vongsangnak et al. 2008). With their assistance, we converted this model to a System Biology Markup Language (SBML) format (Finney and Hucka 2003) that is compatible with open-source FBA software. Our creation of a valid SBML version of the WV1314 *A. oryzae* model should enable us to perform genome-wide simulations of gene deletions to support the genetic engineering of an effective filamentous fungal ethanologen in FY10. Moreover, our conversion of the model to an open-source format will enable others to more easily replicate our results and facilitate collaborative efforts to improve the ethanol production capabilities of *A. oryzae*.

The FBA simulations described above were performed with the open-source COBRA Toolbox (Becker et al. 2007) and the SBML Toolbox (Keating et al. 2006) suites of MATLAB functions. The software models the stoichiometry of all known metabolic transport and reaction pathways within a cellular system or subsystem as a system of linear equations. The units of the fluxes through the pathways are given as millimoles per gram of cellular biomass (dry weight)/per hour. The metabolism of the cell in FBA is assumed to be in a steady state such that the mass fluxes are balanced and sum to zero. One reaction pathway is then assigned to be the objective function of the cell. In FBA simulations of cellular metabolism, the objective function is typically assumed to be the maximization of cellular growth, or, more explicitly, the maximal production of the molecules required to make new cells (Becker et al. 2007).

In performing a particular simulation of metabolism using FBA, one or more transport or reaction fluxes are constrained with upper and lower bounds. The fluxes may also be constrained to be reversible or irreversible, or, in other words, bidirectional or unidirectional within a given metabolic pathway. A linear programming solver is then used to predict the optimal combination of specific fluxes through all pathways that, together, maximize the flux objective function pathway. In this way, FBA methods draw heavily from the field of operations research where problems such as the optimization of airline schedules, delivery routes, or factory outputs are commonplace.

To validate our SBML-formatted version of the WV1314 model for *A. oryzae*, we used the COBRA Toolbox to constrain the glucose uptake flux to 1.2 and the ATP maintenance flux to 1.9. Ammonia, phosphate, and sulfate uptake fluxes were left unconstrained, as were all intracellular and export fluxes. The objective function was defined as maximal growth of cell biomass. Under these conditions, the COBRA Toolbox predicted an optimized growth rate of 0.0993 mmol/g dry weight/hour. A visiting graduate student from the Nielsen group (our collaborators at Chalmers) performed an identical simulation using the proprietary BioOpt software and file format in which the WV1314 model had been originally produced; this resulted in a predicted growth rate of 0.0980 mmol/g DW/hour. The close similarity of these values indicated that our conversion of the WV1314 metabolic network model to valid SBML had been successful. The work of converting the model to a form of SBML compatible with the COBRA Toolbox was challenging and time-consuming, partly because the network contains 729 enzymes, 1314 enzyme-encoding genes, 1073 metabolites, and 1846 biochemical reactions. Moreover, the COBRA Toolbox software was found to contain undocumented requirements for naming metabolites that lie outside the SBML specification (Finney et al. 2003). This made troubleshooting the conversion process difficult and delayed our progress until the problem was discovered.

Using the constraints described in the previous paragraph, we examined the relationship between ethanol output and oxygen uptake in *A. oryzae*. Fermentative ethanol production in fungi is well-known

to require microaerobic, but not completely anaerobic, conditions. To our knowledge, however, the exact oxygen uptake fluxes required for optimal ethanol production by *A. oryzae* have not been defined. We therefore used FBA (using parameters described in the preceding paragraph) to simulate how gradually constraining its oxygen uptake flux may change its predicted ethanol output flux. We also tracked the changes in predicted growth rate for *A. oryzae* when oxygen uptake flux is constrained over identical intervals. Our results indicated that optimal ethanol output occurs within a range of oxygen uptake flux of about 0.1 to 0.01 mmol/g DW/hour (Figure 7.1, left chart). Interestingly, the change in growth rate (Figure 7.1, right chart) appears to plateau across nearly the same range of oxygen uptake flux as that seen for optimal ethanol output flux. The results of the FBA simulation indicated that ethanol output from our fermentation experiments with *A. oryzae* might be easily improved by more closely controlling aeration levels in the fermentation vessels. Moreover, our reasonable results in simulating ethanol production in *A. oryzae* suggest that our FBA software and model are working in a logical manner and should serve us well in FY10 as we move on to performing genome-wide simulations of gene knock-out and overexpression within the COBRA Toolbox to support genetic engineering efforts in this and other tasks of our project.

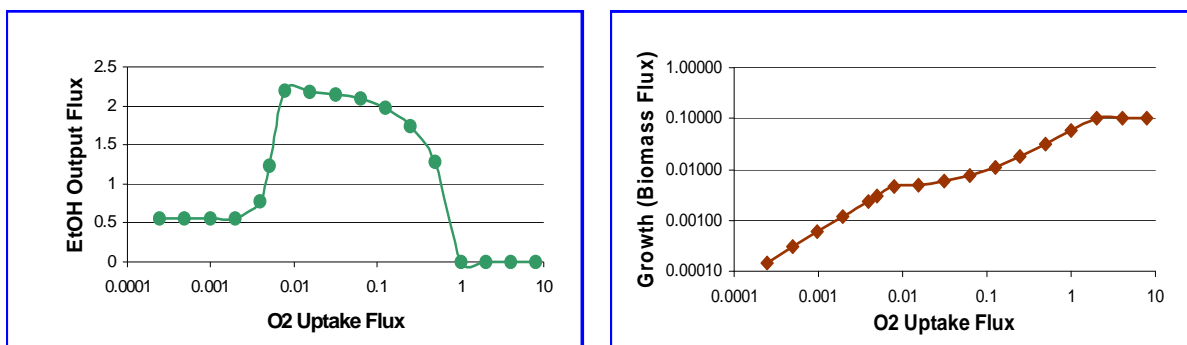


Figure 7.1. (Left chart) Ethanol Output Flux Changes Predicted from FBA of *A. Oryzae* Cellular Metabolism as a Function of Oxygen Uptake Flux. (Right chart) Biomass growth rate changes predicted by FBA of *A. oryzae* cellular metabolism as a function of oxygen uptake flux. Growth is defined as the rate of intracellular accumulation of biomass molecules. The units on both axes of both charts are given as millimoles per gram of cell dry weight per hour.

7.2.2 Fermentation

7.2.2.1 Strain Development

The effort towards *Aspergillus oryzae* transformation and strain development was continued. The first attempts at genetic modifications for improved ethanol production were completed and applied to fermentations. We verified the utility of our previously developed gene knockout system for *A. oryzae* by generating mutants of two genes, *creA* and *alcR*, that are potentially involved in conversion of xylose to ethanol. Homologous recombination was used to substitute the *pyrG* gene for the coding regions of the *A. oryzae* genes for 1) *creA*, mutation of which may prevent repression of a number of genes involved in xylose catabolism and 2) *alcR*, mutation of which prevents interconversion to acetaldehyde and ethanol by alcohol dehydrogenase.

Although we successfully demonstrated our ability to produce knockout mutants in *A. oryzae* using the *creA* and *alcR* genes as model targets, based on the observation that neither of these genes resulted in significant improvement in conversion of simple sugars to ethanol (described below), plans for generation of a *creA/alcR* double mutant were abandoned.

To expand our mutant generation capabilities for *A. oryzae* strain improvements, a method was developed to allow knockouts of multiple genes in a single strain using a recyclable selection marker. This method involved construction of a *pyrG* selection cassette plasmid flanked by direct repeats. Unique sequences at the ends of the cassette allow construction of knockout constructs for any gene in the *A. oryzae* genome. Once a gene has been replaced by the *pyrG* selection cassette, the selection cassette can be removed with recombination between the flanking direct repeats and re-selection for pyrimidine auxotrophy.

Various approaches directed towards alleviating or bypassing the apparent redox imbalance in conversion of xylose to ethanol (as indicated by xylitol accumulation) were investigated for feasibility. Progress on these approaches has included:

- Identification of a xylose isomerase gene from the rumen fungus *Orpinomyces* that could be used to bypass the redox reaction steps in converting xylose to xylulose. To introduce a xylose isomerase gene into *A. oryzae*, a gene encoding the xylose isomerase from *Orpinomyces* was synthesized using the codon preference table for *Aspergillus*. The expression of this gene is driven by the constitutive *A. nidulans* *gapdh* promoter and will be introduced into the *A. oryzae* genome by random integration of a zeocin or *pyrG* selectable plasmid.
- Primers for producing single and double knockout mutants of the native xylose reductase and xylitol dehydrogenase genes were designed and ordered and will be used in conjunction with the recyclable selection marker system described above when it is completed.
- As an alternative approach to alleviate the apparent redox imbalance resulting from the different cofactor preferences of the native *A. oryzae* xylose reductase and/or xylitol dehydrogenase enzymes, a strategy to modify the NAD(P)H cofactor preferences of these enzymes has been developed based on molecular models of the NAD(P)H binding sites in several NAD(P)H requiring enzymes. The regions of the native *A. oryzae* xylose reductase and xylitol dehydrogenase enzymes involved in cofactor binding have been identified based on sequence similarity, and an approach to modify these sites has been designed.

In addition, other potentially problematic side reactions (e.g., ribitol and xylitol formation by non-specific aldose reductases, acetate and lactate formation pathways) that are being identified using metabolic modeling. Strategies to block these side reactions by knockout mutagenesis are also being developed.

7.2.2.2 High-Throughput Screening Method Development

An effort to develop a high-throughput screening method to rapidly identify highly productive fungal ethanologens was initiated. Preliminary investigation of methods to identify individual variants with improved ethanol productivity from a large population was made. An *in vitro* method to detect ethanol production using ethanol oxidase was investigated and found to be useful for moderately high-throughput 96-well arrayed library assays. However, the alcohol oxidase enzyme was not sufficiently stable for use in very high-throughput plate assays.

Microtiter plate-based assays allow screening of several thousand variants, but these variants must first be picked and arrayed into the 96 well format. In contrast, culture plate-based assays do not require picking and arraying and can therefore be adapted to screen hundreds of thousands of genetic variants, greatly increasing the chances of finding useful mutations. To develop a very high throughput culture plate bioassay to screen for improved ethanol production by filamentous fungi, five ethanol-responsive promoters from the *E. coli* genes *dnaK*, *grpE*, *katG*, *pgaA*, and *uspA* were fused with the reporter gene *LacZ*-alpha in a pBS KS (+) plasmid background, sequenced and transformed into *E. coli* (Figure 7.2).

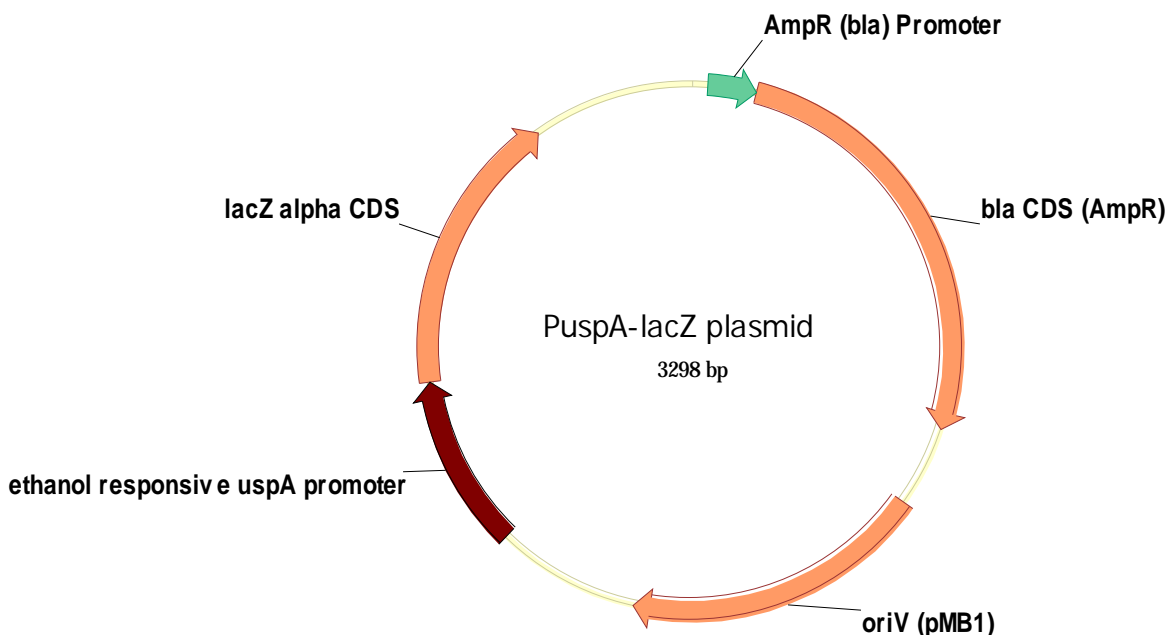


Figure 7.2. Ethanol Responsive Promoters from the *E. coli* Genes *dnaK*, *grpE*, *katG*, *pgaA*, and *uspA* Fused with Reporter Gene *LacZ*-Alpha in a pBS KS (+) Plasmid Background, Sequenced and Transformed into *E. Coli*

The resulting *E. coli* strains were tested for *lacZ* expression in response to ethanol under bioassay plate conditions. All were responsive to ethanol at 2% to some degree, but the response was most evident with the *grpE*-*lacZ* and *uspA*-*lacZ*. However, these promoters also showed a fairly high level of background expression at stationary phase in the absence of ethanol. We then tested the ethanol gradient responsiveness of this bacterial bioassay. The expected result was the development of larger zones of *lacZ* expression around higher concentrations of ethanol. At lower concentrations of ethanol (<3%), this appeared to be true, but at ethanol concentrations above 3%, there was no evidence of expression with any of these promoters. Control experiments with the constitutive *lacZ* promoter driving expression of *lacZ* demonstrated expression at ethanol concentrations up to ~5%, indicating that *lacZ* is active at higher ethanol concentrations. Three of the promoter constructs, (*dnaK*-*lacZ*, *katG*-*lacZ*, and *uspA*-*lacZ*) showed expression of *lacZ* at stationary phase in the absence of ethanol, but this stationary phase expression was completely repressed at 3% ethanol.

A further finding was that growth of the *E. coli* host strain was uniform up to 3% ethanol, but was completely inhibited at 6% ethanol. This led to the conclusion that this system may still be viable as a bioassay for ethanol, although not in the way that was originally envisioned. The bioassay as currently

envisioned will use 1) activation of lacZ expression in exponentially growing cells up to 2% ethanol, 2) repression of lacZ expression at stationary phase for ethanol concentrations up to 5%, and 3) growth repression of the *E. coli* host above 5%. The uspA-lacZ construct was judged to be the most efficacious for this purpose, and further tests are being performed with this construct.

In the event that the bioassay continues to prove useful, a strategy for replacing the lacZ reporter in the uspA-lacZ construct with the fluorescent egfp reporter was developed, and the primers to accomplish this were designed. This substitution will increase the speed and sensitivity of this assay and eliminate the need for the expensive lacZ.

Although the plate-based bioassay system still appears to have potential, concerns about the dynamic range of this assay and variability in response prompted us to continue development of a moderate throughput assay for ethanol production using an alcohol oxidase-based detection system. Results indicate that this system can easily be adapted to the 96 well format.

To generate the mutant population of *A. oryzae* that can be screened for mutations affecting ethanol production using the above methods, an *Agrobacterium*-based mutagenesis system is being developed. A T-DNA vector for fungal transformation was developed in-house from the plant transformation vector pBIN101. This vector is being further modified to use the pyrG selection system required for use in *A. oryzae*. We are currently developing a generally useful T-DNA vector for concomitant generation of an insertional knockout mutant library and an expressional trapping library. This approach uses a T-DNA region that contains the *A. fumigatus* pyrG gene to allow T-DNA integration events to be selected and also contains an outwardly directed *A. nidulans* gapd promoter adjacent to the right T-DNA border. Using this system, T-DNA insertions within coding sequences, or those disrupting native promoters, will yield loss of function mutants while insertions that place the T-DNA-derived gapdh promoter upstream of a coding sequence will result in constitutive overexpression of that gene. This will allow us to capture both null and over-expression phenotypes in a single library. Established protocols for *Agrobacterium* transformations were obtained from the literature and have been demonstrated to be functional in our laboratory.

7.2.2.3 Fermentation Results

Fermentation work initiated in FY08 continued in FY09 in support of the ethanol development effort. Fermentations were conducted at 0.1, 0.5, and 20-liter working volumes to establish ethanol production baseline values for glucose, xylose, and glucose/xylose mix media and to discover experimental conditions that would decrease variability in the fermentation data so that valid evaluations of strain modifications would be possible. It was discovered that increasing the level of inoculation decreased data variability considerably. Increasing vent size from 1/16 in. ID to 3/16 in. ID on 250-mL flasks was found to increase ethanol production levels. These experimental conditions were applied to fermentations to establish new baselines for ethanol production and to compare the *A. oryzae* NRRL 697 parental strain to our newly generated *creA* and *alcR* mutants. Experiments showed that the two mutants produce slightly less ethanol than the parent strain. On 12% glucose medium, the *alcR* mutant and *creA* mutants produced 1.6% and 7.6% less ethanol, respectively, than the parent strain (Figure 7.3).

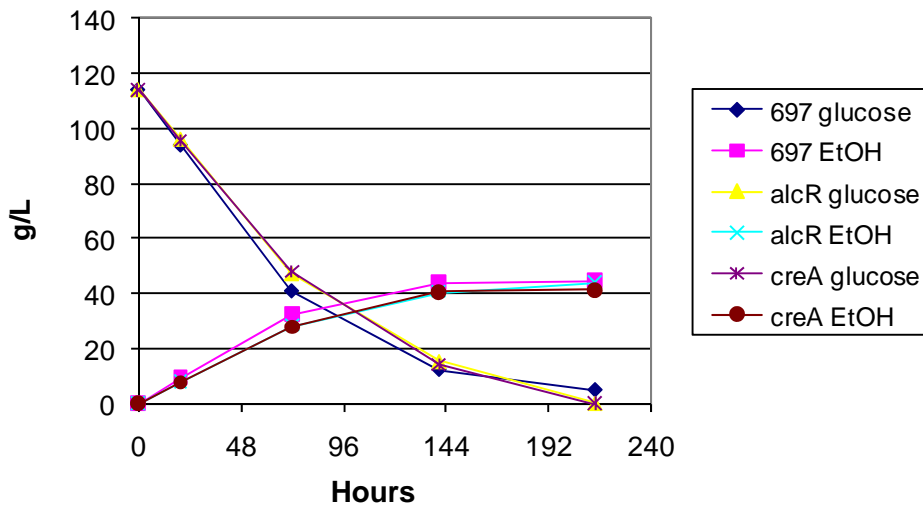


Figure 7.3. Exp 40, *A. oryzae* NRRL 697, *alcR* and *creA* Mutants Ethanol Production on 12% Glucose Minimal Medium Enriched with 0.5% Yeast Extract (averages for nine replicates)

On 12% xylose medium, the *alcR* and *creA* mutants produced 3.2% and 10.1% less ethanol, respectively, than the parent strain (Figure 7.4).

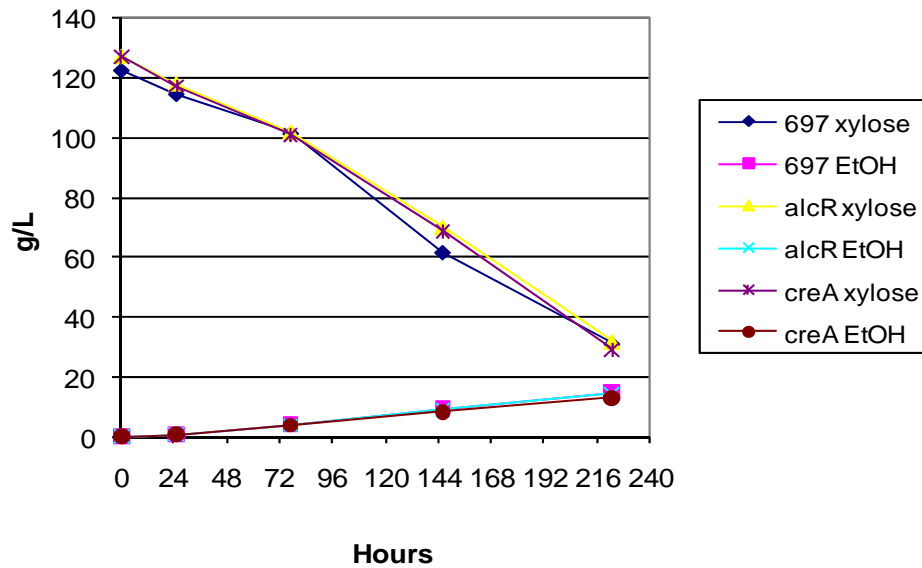


Figure 7.4. Exp 42, *A. oryzae* NRRL 697, *alcR* and *creA* Mutants Comparison for Ethanol Production on 12% Xylose Minimal Medium Enriched with 0.5% Yeast Extract (averages for nine replicates)

Neither of these strain modifications enhanced ethanol production. To provide scale-up data, 20-L working volume fermentations in 30-L fermentors were completed to establish baseline values for ethanol titers and production rates on glucose, xylose, or glucose/xylose media using the *A. oryzae* model strain. Ethanol titer of 3.9% was achieved in 4 days from 12% glucose minimal medium enriched with

0.5% yeast extract when using an initial spore titer of 5×10^5 spores/mL. Applying what was learned in the flask experiments about inoculation levels to the fermentor, we conducted an experiment using the much higher spore titer of 2×10^7 spores/mL and achieved a similar ethanol titer of 3.85% in only 3 days (Figure 7.5).

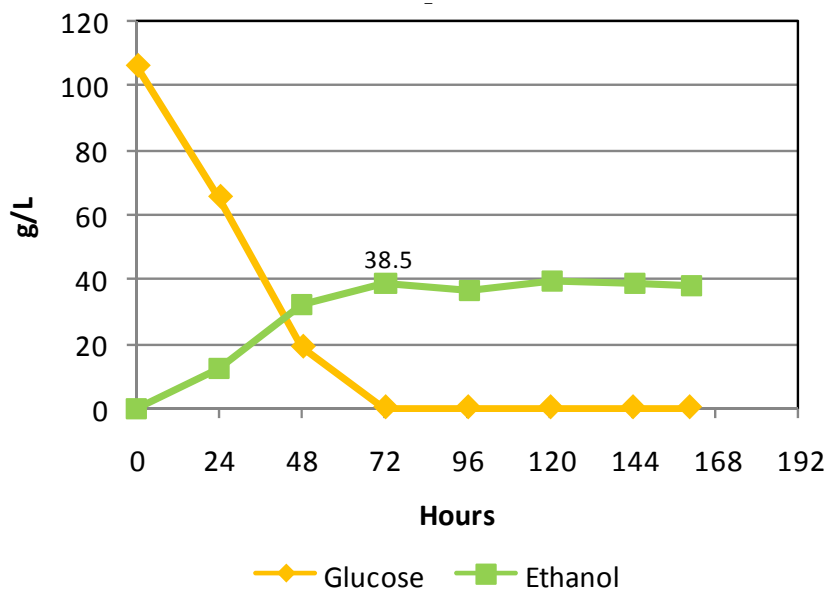


Figure 7.5. Exp 51, *Aspergillus oryzae* NRRL 697 Model Strain Ethanol Production on 12% Glucose Minimal Medium Enriched with 0.5% Yeast Extract, 20-Liter Working Volume, and 2×10^7 Spores/mL

When xylose was used as the carbon source in the fermentor, an ethanol titer of 5.9 g/L was achieved in 9 days from an initial spore titer of 5×10^5 spores/mL. When the initial spore titer was increased to 2×10^7 spores/mL, an ethanol titer of 9.96 g/L was reached in 8 days (Figure 7.6). Xylitol reached 39.6 g/L by Day 7 (Figure 7.6) and gradually declined to 0.91 g/L by Day 24 (not shown).

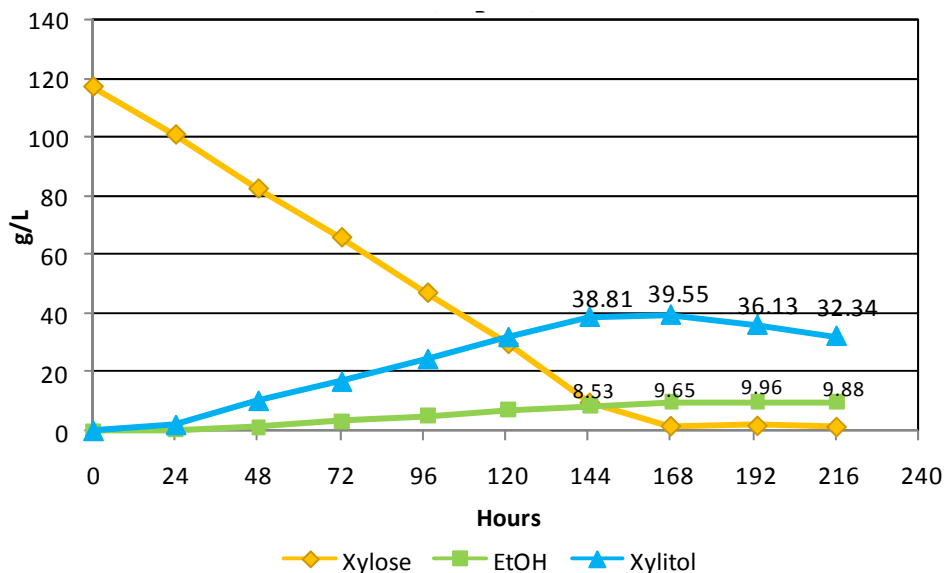


Figure 7.6. Exp 49, *A. oryzae* NRRL 697 Model Strain on Ethanol Production on 12% Glucose Minimal Medium Enriched with 0.5% Yeast Extract, 20-Liter Working Volume, and 2×10^7 Spores/mL

Avoiding the formation of significant amounts of xylitol or quickly converting what is formed to ethanol is key to developing an effective *A. oryzae* based ethanologen for the conversion of xylose. To provide additional background information for our strain modification effort, a flask experiment using five replicate 250-mL flasks containing 100 mL of working volume was conducted. The medium was 40 g/L xylitol minimal medium enriched with 0.5% yeast extract. With xylitol as the primary carbon source, the 40 g/L xylitol was converted by Day 12 (Figure 7.7). Only at or below detection limit concentrations of acetic acid and ethanol were detected by high-performance liquid chromatography (HPLC) analysis. Nuclear magnetic resonance (NMR) analysis indicated that formate, pyruvate, and succinate were also present, but further analysis is required to quantify these co-products.

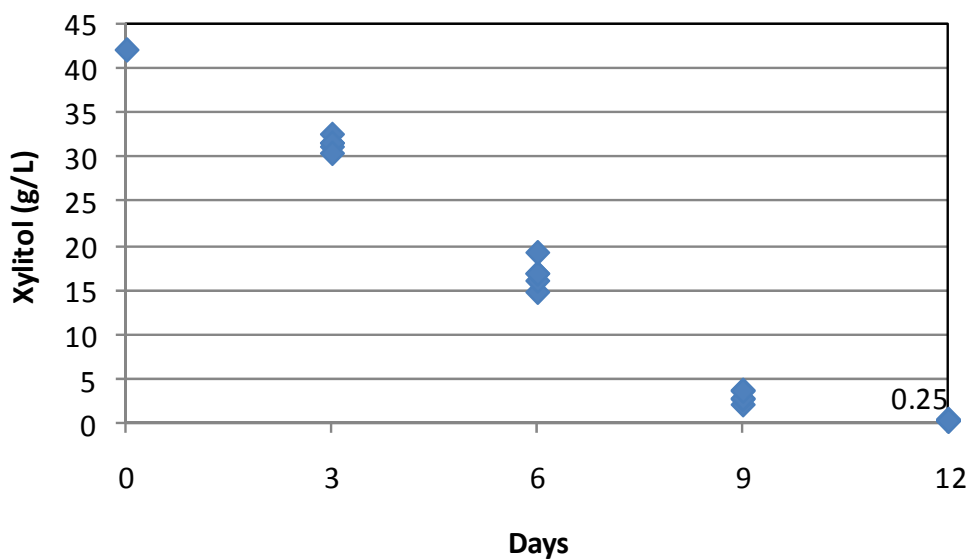


Figure 7.7. Exp 46, Xylitol Remaining from *A. oryzae* NRRL 697 Model Strain on 4% Xylitol Minimal Medium Enriched with 0.5% Yeast Extract, 250-mL flasks, 100 mL of working volume, and 2×10^7 spores/mL

A readily available and inexpensive material from an ethanol production process showed positive results when used as media enrichment to enhance ethanol yields for glucose and xylose conversions. Thin stillage from two distinctly different commercial operations both provided nutrients that enhanced the conversion of glucose and xylose (Figure 7.8). For glucose conversion, 0.5% yeast extract as a nutrient enrichment outperformed the 10% thin stillage enrichments slightly.

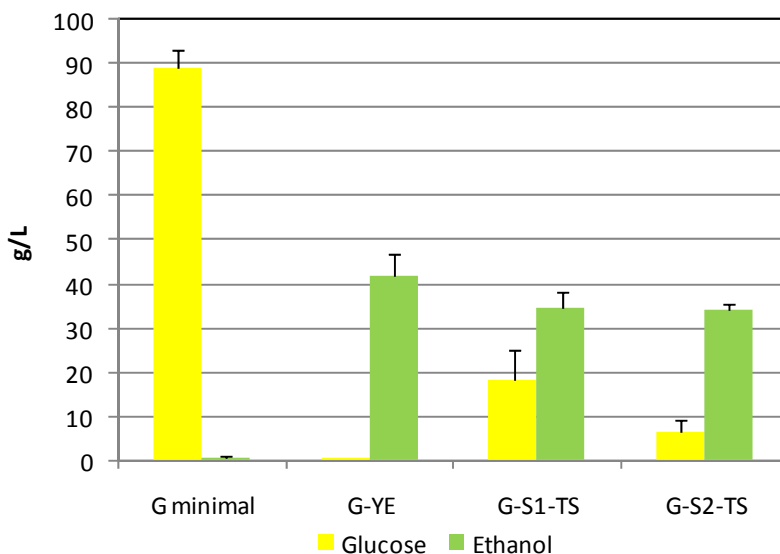


Figure 7.8. Exp 44, *A. oryzae* NRRL 697 Model Strain Ethanol Production on 12% Glucose Minimal Medium Enriched with 0.5% Yeast Extract, or 10% Source 1 Thin Stillage or 10% Source 2 Thin Stillage, 250-mL flasks, 100 mL of working volume, and 2×10^7 spores/mL

However, the positive effect of thin stillage enrichment on xylose conversion was more pronounced, with 10% thin stillage providing better xylose conversion results than 0.5% yeast extract (Figure 7.9). More ethanol was produced, less xylose was consumed, and less xylitol was produced. An invention report was submitted for review.

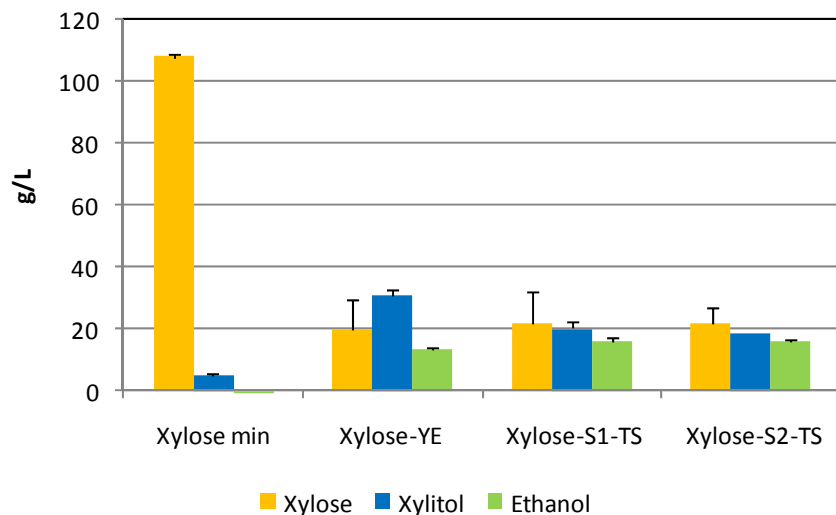


Figure 7.9. Exp 44, *A. oryzae* NRRL 697 Model Strain Ethanol Production on 12% Xylose Minimal Medium Enriched with 0.5% Yeast Extract, or 10% Source 1(S1) Thin Stillage or 10% Source 2 (S2) Thin Stillage, 250-mL flasks, 100 mL of Working Volume, and 2×10^7 spores/mL

A method using rice and autoclavable plant tissue culture bags to easily and inexpensively produce large numbers of *A. oryzae* conidia for inoculation of the fermentors was developed. Using this method, one bag produces enough conidia to inoculate a fermentor at a small fraction of the labor and material costs associated with the previous plate-based production method.

7.3 Plans for FY2010

- Refine high-throughput screening method and create ethanol screening protocol. Continue to identify individual genes for ethanol production improvement and combine them to create a novel production strain and then establish baseline production levels on glucose, xylose, and complex biomass.
- Identify individual genes that improve ethanol tolerance in filamentous fungi using genome-wide gene knock-out and overexpression methods or other screening methods and apply to the model strain.
- Improve ethanol tolerance in the novel production strain by single or multiple gene modifications and/or applying screening methods.

8.0 Major Subtask A.6 Alternative Renewable Fuels from Fungi

8.1 Background

The purpose of this subtask is to explore fungi as sources of alternative renewable fuels. We are interested in advanced biofuel molecules, i.e., those molecules that are infrastructure compatible. Beginning in FY10, we will identify promising fungi, enzymes, or pathways and perform proof-of-principle experiments to research possible routes to advanced biofuels.

8.2 Accomplishments and Results

In FY09, we performed a broad assessment of potential fungal routes to alternative renewable fuels. In regard to advanced biofuels, the primary compounds of interest are hydrocarbon or hydrocarbon-like compounds. Potential biofuel molecules would have the following desirable properties: low oxygen content, low water solubility, and high degree of saturation—in short, they would be infrastructure compatible fuels. Fungi can produce hydrocarbon or hydrocarbon-like compounds from a variety of pathways (Table 8.1). These include 1) fatty acid synthesis leading to triglycerides, 2) the isoprenoid pathway leading to compounds that are multiples of five carbon units from C₁₀ to C₄₀, 3) polyketide synthases that produce an amazing array of compounds of varying degrees of cyclization and functionalization, and 4) hydrocarbon compounds from C₄ to C₃₆ that may be produced by various mechanisms (Ladygina et al. 2006).

Table 8.1. Classes of Hydrocarbon and Hydrocarbon-Like Molecules Produced by Fungi

Compound	No. of Carbons	Key Enzyme(s)
Fatty acids, triglycerides	C ₁₂ – C ₂₂	fatty acid synthases
Fatty alcohols	C ₁₂ – C ₂₂	acyl-reductases
Polyketides	C _{(2n)+1} ; C ₉ – C ₆₅	polyketide synthases, oxidases, modifying enzymes
Terpenes (isoprenoids)	C _{5n} ; C ₁₀ – C ₄₀	terpene synthases, modifying enzymes
Alkanes, cycloalkanes	C ₄ – C ₃₆	acyl-reductases, thioesterases, decarbonylase, others?

It has been known for years that certain fungal species, including both yeasts and filamentous fungi, can produce and accumulate large amounts of lipids when grown on various carbon sources, including diverse sugars (Suzuki and Hasegawa 1974; Ratledge 2002; Fakas et al. 2009). These oil-producing (oleaginous) fungi accumulate triglycerides of varying fatty acid composition and/or carotenoids, which are 40-carbon compounds produced via the isoprenoid pathway. Some example genera of oleaginous or carotenogenic yeasts are *Lipomyces*, *Debaryomyces*, *Rhodotorula*, *Candida*, *Yarrowia* and *Hansenula*; and filamentous fungi *Cunninghamella*, *Mortierella*, *Mucor*, *Blakeslea*, and *Phycomyces* (all zygomycetes).

The oleaginous fungi are not the species of primary interest in this task, at least in regard to the triglycerides that they produce. However, these species might serve as platform organisms to over-produce hydrocarbons if the pathways to the hydrocarbons are identified and engineered into the oleaginous species. This assumes that these oleaginous strains can be genetically manipulated; this is

certainly the case for many of the yeasts and at least one of the filamentous fungi named above (Ando et al. 2009). Using these oleaginous fungi as platforms would be potentially beneficial for two reasons. First, many fungal-derived hydrocarbons are generated by a few additional steps after fatty acid synthesis; thus, it follows that fatty acid anabolism will be crucial to generating large quantities of the hydrocarbons. Second, these oleaginous fungi already have mechanisms for accumulating and tolerating high concentrations of lipophilic compounds, so they might be well-equipped to accumulate high concentrations of hydrocarbons. This is important since high concentrations of hydrocarbons may be toxic to the native fungal producers of the hydrocarbons.

Even more intriguing, given our interest in alternative biofuels, are the examples of fungi producing one or more alkanes. These may arise from the fatty acid decarbonylation pathway, via the isoprenoid pathway, or some other undetermined route of biosynthesis. The decarbonylation route involves multiple enzymes, including acyl-coenzyme A (acyl-CoA) reductases, thioesterases and decarbonylase (Schneider-Belhaddad and Kolattukudy 2000). The result of this is the production of a hydrocarbon that is one carbon shorter than the starting fatty acid. *Hormoconis resiniae* (aka *Cladosporium resiniae*) is an example of a fungus capable of producing alkanes from C₇ to C₃₆ while growing heterotrophically on glucose or glutamic acid (Walker and Cooney 1973). This fungus is now the subject of a genome sequencing project in a collaboration involving PNNL, the DOE Office of Science (DOE-SC) funded Joint BioEnergy Institute (JBEI) and JGI. Quite recently, the fungus *Gliocladium roseum* was isolated and its suite of hydrocarbons characterized (Strobel et al. 2008). Volatile compounds are produced by a variety of fungi, including species of the cosmopolitan fungal genera *Penicillium* and *Aspergillus*. They produce a range of volatiles, including hydrocarbons, short chain alcohols, ketones, ethers, esters, and terpenes (Sunesson et al. 1995). All of these fungi accumulate rather low levels of the desirable hydrocarbons, and the biochemistry and genetics underlying the production of these compounds remains relatively poorly understood.

Polyketides are a large family of molecules generally produced by condensation of successive malonyl-CoA units. The large enzymes responsible for the production of polyketides are called polyketide synthases (PKSs). PKSs consist of multiple catalytic domains carrying out acyl transfer, ketoreductase, dehydratase, thioesterase, and other functions. Fungal polyketide synthases are referred to as iterative type I PKSs since they have the multiple catalytic domains on a single polypeptide chain, and the growing polyketide molecule may be passed through the catalytic domains more than once (Cox and Simpson 2009). The other interesting feature of polyketide synthesis in fungi is that PKSs and the associated modifying enzymes exist in gene clusters. This is the norm in the bacterial domain, but is largely restricted to secondary metabolite clusters, such as polyketides, isoprenoids, and non-ribosomal peptides, in fungi. The polyketide synthases and their associated modifying enzymes are basically one of nature's combinatorial chemistry toolboxes. Polyketides have a wide range of sizes from C₉ to C₆₅ and beyond. They also have a wide range of types and numbers of functional groups, including keto and hydroxyl groups, double and triple bonds, cycloalkane, cyclic ether, and aromatic groups. Some of these groups are introduced by accessory enzymes associated with the PKS gene clusters, such as cytochrome P450s. Since the goal from a biofuels perspective would be to generate molecules with relatively low levels of oxygen, we would like to identify PKSs that generate highly reduced polyketides. Since many polyketides are aromatic, they may also be potential fuel modifiers, e.g., octane boosters. In addition, the partially oxygenated polyketides could be alternative fuel oxygenates.

Isoprenoids are synthesized in fungi via the mevalonate pathway, which involves the condensation of activated C₅ units (isopentenyl pyrophosphate and dimethylallyl pyrophosphate) derived from mevalonate

to form a diverse family of higher molecular weight compounds (Scott et al. 2004, pp. 163-198). These include C₁₀ (monoterpenes), C₁₅ (sesquiterpenes), C₂₀ (diterpenes), C₃₀ (squalenes), and C₄₀ (carotenoids) compounds. The family of isoprenoid compounds that include linear and cyclized molecules are formed by specific terpene synthases (Keeling and Bohlmann 2006). Subsequently, some of these molecules are further modified by accessory enzymes (Hamberger and Bohlmann 2006). The family of C₁₀ and C₁₅ compounds would be of greatest interest since they are in the size range of molecules found in diesel, Jet-A, or JP-8 fuels. Larger isoprenoids could potentially be catalytically cracked to smaller molecules in the gasoline to diesel/jet fuel range.

The diversity of hydrocarbon and hydrocarbon-like compounds produced by fungi holds great promise for identifying advanced biofuels. Some of the research challenges awaiting us are to identify the top candidate biofuel molecules and the pathways leading to the production of those molecules and to either manipulate fungal culture conditions or genetically manipulate the production organism to increase the production of the alternative biofuel molecule(s) into the economically relevant range.

8.3 Plans for FY10

In FY10, we will begin experimental work in three areas: terpene production, polyketide clusters as sources of biomolecules or modifying enzymes, and the genomics of hydrocarbon-producing fungi. Based on results of this fiscal year's experiments and analyses, we expect to develop a sharper focus on particular systems for more intensive study in out-years.

The hydrocarbon-producing fungi are ripe targets for further study. Specifically, genomics, transcriptomics, and proteomics studies would facilitate the discovery of enzymes and pathways. Genetic manipulation of fungi via knockout or over-expression of candidate genes identified via the genomic studies would be a natural follow-up. If molecular biological tools to manipulate the native host could be developed, then gene knockouts could proceed in this organism. Initially, we would plan on over-expressing acyl reductase and decarboxylase genes in one of our platform organisms, e.g., *A. niger* or *A. terreus*. These experiments in a non-hydrocarbon producing strain would help to confirm the pathways and/or create hydrocarbon over-producing strains. These studies would await the completion of the *H. resinae* genome and transcriptome sequencing. Therefore, the immediate goal for FY10 is to culture *H. resinae* for preparation of DNA for genome sequencing and RNA from a variety of conditions for transcriptome (expressed sequence tag; EST) sequencing. Further research on this organism or the genes is anticipated to begin at the end of FY10 or beginning of FY11 as the genome resources become available.

Accessory enzymes that reduce and dehydrate the growing polyketides could be useful for producing modified polyketides or modifying other potential fuel molecules of interest, starting with feedstock molecules that are not derived from PKSs; i.e., enzymatic deoxygenation of polyols. Efforts in the general area of studying PKSs and the associated modifying enzymes will build on an existing collaboration with Clay Wang of the University of California-Los Angeles, who is experienced in the analysis of PKS clusters and the products they produce (Chiang et al. 2008). The goal of this project will be to develop enzymes that can enhance the energy content or otherwise favorably alter organic compounds that are used as advanced biofuels. PKS gene clusters are often "silent" or expressed at very low levels in culture. Strains will be constructed that induce the expression of these PKS and modifying enzyme genes so that we can screen for novel polyketides and enzyme activities. A portion of the project

will be dedicated to finding appropriate organic compounds that are both relevant to biofuel production and amenable to screening. Examples are the thermochemical biomass pretreatment by-products levulinic acid, furfural and hydroxymethylfurfural, or their reduced alcohol counterparts. These compounds or their derivatives are potential biofuels and also known inhibitors of fermentation processes, so the identification of enzymes to modify them would have two potential benefits/applications. In out-years, we will build upon the diversity of organic compound modifying enzymes present in fungi by creating pooled expression libraries of these genes containing random mutations. The libraries will then be screened for changes in substrate specificity. Ultimately, enzymes with activity on compounds from advanced biofuel production can be discovered by inducing the expression of these genes and then modifying them to be active on target substrates.

Beginning in FY10, we will genetically manipulate one of our model organisms, *Aspergillus niger*, to produce a monoterpene (C₁₀) by incorporating a terpene synthase gene alone or in combination with a geranyl diphosphate synthase gene to increase the concentration of substrate (geranyl diphosphate) for the terpene synthase. Active expression of the enzymes will be assessed by specific enzyme assays. Production of the desirable terpenes will be determined by gas chromatographic analysis.

9.0 References

- Ando A, Y Sumida, H Negoro, DA Suroto, J Ogawa, E Sakuradani, and S Shimizu. 2009. "Establishment of *Agrobacterium tumefaciens*-Mediated Transformation of an Oleaginous Fungus, *Mortierella alpina* 1S-4, and Its Application for Eicosapentaenoic Acid Producer Breeding." *Applied and Environmental Microbiology* 75(17):5529-5535.
- Becker SA, AM Feist, ML Mo, G Hannum, BO Palsson, and MJ Herrgard. 2007. "Quantitative prediction of cellular metabolism with constraint-based models: the COBRA Toolbox." *Nat. Protocols* 2(3):727-738.
- Bergmeyer HU, M Grassl, and HE Walter. 1985. "Biochemical reagents for general use: Enzymes." In: (3rd ed.), HU Bergmeyer, Editor, *Methods of Enzymatic Analysis*, Vol. 2, Verlag Chemie, Weinheim.
- Chiang YM, E Szewczyk, T Nayak, AD Davidson, JF Sanchez, HC Lo, WY Ho, H Simityan, E Kuo, A Praseuth, K Watanabe, BR Oakley, and CCC Wang. 2008. "Molecular genetic mining of the *Aspergillus* secondary metabolome: discovery of the emericellamide biosynthetic pathway." *Chemistry & Biology* 15(6):527-532.
- Colot HV, G Park, GE Turner, C Ringelberg, CM Crew, L Litvinkova, RL Weiss, KA Borkovich, and JC Dunlap. 2006. "A high-throughput gene knockout procedure for *Neurospora* reveals functions for multiple transcription factors." In: *Proceedings of the National Academy of Sciences of the United States of America* 103(27):10352-10357.
- Conrads TP, GA Anderson, TD Veenstra, L Pasa-Tolić, and RD Smith. 2000. "Utility of Accurate Mass Tags for Proteome-Wide Protein Identification." *Analytical Chemistry* 72(14):3349-3354.
- Cox RJ and TJ Simpson. 2009. "Fungal Type I Polyketide Synthases. Complex Enzymes in Microbial Natural Product Biosynthesis, Part B: Polyketides." *Aminocoumarins and Carbohydrates* 459:49-78.
- Daly DS, KK Anderson, EA Panisko, SO Purvne, R Fang, MM Monroe, and SE Baker. 2008. "Mixed-Effects Statistical Model for Comparative LC-MS Proteomic Studies." *Journal of Proteome Research* 7:1209-1217.
- Fakas S, S Papanikolaou, A Batsos, M Galiotou-Panayotou, A Mallouchos, and G Aggelis. 2009. "Evaluating renewable carbon sources as substrates for single cell oil production by *Cunninghamella echinulata* and *Mortierella isabellina*." *Biomass & Bioenergy* 33(4):573-580.
- Finney A and M Hucka. 2003. "Systems biology markup language: Level 2 and beyond." *Biochem. Soc. Trans.* 31(6):1472-1473.
- Gao J, GJ Opiteck, MS Friedrichs, AR Dongre, and SA Hefta. 2003. "Changes in the Protein Expression of Yeast as a Function of Carbon Source." *Journal of Proteome Research* 2(6):643-649.
- Gems D, IL Johnstone, and AJ Clutterbuck. 1991. "An Autonomously Replicating Plasmid Transforms *Aspergillus-Nidulans* at High-Frequency." *Gene* 98(1):61-67.

- Gygi SP, B Rist, SA Gerber, F Turecek, MH Gelb, and R Aebersold. 1999. "Quantitative Analysis of Complex Protein Mixtures Using Isotope-Coded Affinity Tags." *Nature Biotechnology* 17(10):994-999.
- Hamberger B and J Bohlmann. 2006. "Cytochrome P450 mono-oxygenases in conifer genomes: discovery of members of the terpenoid oxygenase superfamily in spruce and pine." *Biochemical Society Transactions* 34:1209-1214.
- Keeling CI and J Bohlmann. 2006. "Genes, enzymes and chemicals of terpenoid diversity in the constitutive and induced defence of conifers against insects and pathogens." *New Phytologist* 170(4):657-675.
- Keating SM, BJ Bornstein, A Finney, and M Hucka. 2006. "SBMLToolbox: an SBML toolbox for MATLAB users." *Bioinformatics* 22(10):1275-7.
- Ladygina N, EG Dedyukhina, and MB Vainshtein. 2006. "A review on microbial synthesis of hydrocarbons." *Process Biochemistry* 41(5):1001-1014.
- Magnuson JK and LL Lasure. 2004. *Organic Acid Production by Filamentous Fungi*. In: *Advances in Fungal Biotechnology for Industry, Agriculture and Medicine*, J. Tkacz (ed.), Kluwer Academic Publishers.
- Meyer V, M Arentshorst, A El-Ghezal, AC Drews, R Kooistra, CAMJJ van den Hondel, and AFJ Ram. 2007. "Highly efficient gene targeting in the *Aspergillus niger* kusA mutant." *Journal of Biotechnology* 128(4):770-775.
- Meyer V, M Arentshorst, CAMJJ Van den Hondel, and AFJ Ram. 2008. "The polarisome component SpaA localises to hyphal tips of *Aspergillus niger* and is important for polar growth." *Fungal Genetics and Biology* 45(2):152-164.
- Moorthamer M and B Chaudhuri. 1999. "Identification of Ribosomal Protein L34 as a Novel Cdk5 Inhibitor." *Biochemical and Biophysical Research Communications* 255(3):631-638.
- Nielsen JB, ML Nielsen, and UH Mortensen. 2008. "Transient disruption of non-homologous end-joining facilitates targeted genome manipulations in the filamentous fungus *Aspergillus nidulans*." *Fungal Genetics and Biology* 45(3):165-170.
- Ninomiya Y, K Suzuki, C Ishii, and H Inoue. 2004. "Highly efficient gene replacements in *Neurospora* strains deficient for nonhomologous end-joining." In: *Proceedings of the National Academy of Sciences of the United States of America* 101(33):12248-12253.
- Piddington CS, CS Houston, M Paloheimo, M Cantrell, A Miettinen-Oinonen, H Nevalainen, and J Rambosek. 1993. "The cloning and sequencing of the genes encoding phytase (phy) and pH 2.5-optimum acid phosphatase (aph) from *Aspergillus niger* var. *awamori*." *Gene* 133: 55-62.
- Ratledge C. 2002. "Regulation of lipid accumulation in oleaginous micro-organisms." *Biochemical Society Transactions* 30:1047-1050.

- Rocha I, J Forster, and J Nielsen. 2008. "Design and application of genome-scale reconstructed metabolic models." *Methods Mol Biol.* 416:409-31.
- Schneider-Belhaddad F and P Kolattukudy. 2000. "Solubilization, partial purification, and characterization of a fatty aldehyde decarboxylase from a higher plant, *Pisum sativum*." *Archives of Biochemistry and Biophysics* 377(2):341-349.
- Scott DB, GB Jameson, and EJ Parker. 2004. *Isoprenoids: Gene Clusters and Chemical Puzzles. Advances in Fungal Biotechnology for Industry, Agriculture, and Medicine.* JS Tkacz and L Lange. Kluwer Academic/Plenum Publishers, New York.
- Strobel GA, B Knighton, K Kluck, YH Ren, T Livinghouse, M Griffin, D Spakowicz, and J Sears. 2008. "The production of myco-diesel hydrocarbons and their derivatives by the endophytic fungus *Gliocladium roseum* (NRRL 50072)." *Microbiology-Sgm* 154:3319-3328.
- Sunesson A-L, WHJ Vaes, C-A Nilsson, G Blomquist, B Andersson, and R Carlson. 1995. "Identification of Volatile Metabolites from Five Fungal Species Cultivated on Two Media." *Applied and Environmental Microbiology* 61(8):2911-2918.
- Suzuki T and K Hasegawa. 1974. "Variations in Lipid Compositions and in Lipid Molecular Species of *Lipomyces-Starkeyi* Cultivated in Glucose Sufficient and Glucose Deficient Media." *Agricultural and Biological Chemistry* 38(AUG):1485-1492.
- Vongsangnak W, P Olsen, K Hansen, S Krogsgaard, and J Nielsen. 2008. "Improved annotation through genome-scale metabolic modeling of *Aspergillus oryzae*." *BMC Genomics* 9:245.
- Walker JD and JJ Cooney. 1973. "Aliphatic Hydrocarbons of *Cladosporium resinae* Cultured on Glucose, Glutamic Acid and Hydrocarbons." *Applied Microbiology* 26(5):705-708.
- Wilkins MR, Pasquali C, Appel RD, Ou K, Golaz O, Sanchez JC, Yan JX, Gooley AA, Hughes G, Humphery-Smith I, Williams KL, Hochstrasser DF. 1996. "From Proteins to Proteomes: Large Scale Protein Identification by Two-Dimensional Electrophoresis and Amino Acid Analysis." *Bio-Technology* 14(1):61-65.

10.0 Publications

D Martinez, J Challacombe, I Morgenstern, D Hibbett, M Schmoll, CP Kubicek, P Ferreira, FJ Ruiz-Duenas, AT Martinez, P Kersten, KE Hammel, A Vanden Wymelenberg, J Gaskell, E Lindquist, G Sabat, SS Bondurant, LF Larrondo, P Canessa, R Vicuna, J Yadav, H Doddapaneni, V Subramanian, AG Pisabarro, JL Lavín, JA Oguiza, E Master, B Henrissat, PM Coutinho, P Harris, JK Magnuson, SE Baker, K Bruno, W Kenealy, PJ Hoegger, U Kües, P Ramaiya, S Lucas, A Salamov, H Shapiro, H Tu, CL Chee, M Misra, G Xie, S Teter, D Yaver, T James, M Mokrejs, M Pospisek, IV Grigoriev, T Brettin, D Rokhsar, R Berka, and D Cullen. 2009. “Genome, transcriptome, and secretome analysis of wood decay fungus *Postia placenta* supports unique mechanisms of lignocellulose conversion.” 2009. In: *Proc Natl Acad Sci U S A*. Feb10;106(6):1954-9. Epub 2009 Feb 4. PubMed PMID: 19193860; PubMed Central PMCID: PMC2644145.

Diego Martinez JC, I Morgenstern, D Hibbett, M Schmoll, CP Kubicek, P Ferreira, FJ Ruiz-Duenas, AT Martinez, P Kersten, KE Hammel, AV Wymelenberg, J Gaskell, E Lindquist, G Sabat, SS BonDurant, LF Larrondo, P Canessa, R Vicuna, J Yadav, H Doddapaneni, V Subramanian, AG Pisabarro, JL Lavín, JA Oguiza, E Master, B Henrissat, PM Coutinho, P Harris, JK Magnuson, SE Baker, K Bruno, W Kenealy, PJ Hoegger, U Kües, P Ramaiya, S Lucas, A Salamov, H Shapiro, H Tu, CL Chee, M Misra, G Xie, S Teter, D Yaver, T James, M Mokrejs, M Pospisek, IV Grigoriev, T Brettin, D Rokhsar, R Berka, and D Cullen. 2009. “Genome, transcriptome, and secretome analysis of wood decay fungus *Postia placenta* supports unique mechanisms of lignocellulose conversion.” In: *Proceedings of the National Academy of Sciences* 106(6):1954-1959.

Jovanovic I, JK Magnuson, F Collart, B Robbertse, WS Adney, ME Himmel, and SE Baker. 2009. “Fungal glycoside hydrolases for saccharification of lignocellulose: outlook for new discoveries fueled by genomics and functional studies.” *Cellulose* 16(4):687-697.

Le Crom S, W Schackwitz, L Pennacchio, JK Magnuson, DE Culley, JR Collett, J Martin, IS Druzhinina, H Mathis, F Monot, B Seiboth, B Cherry, M Rey, R Berka, CP Kubicek, SE Baker, and A Margeot. 2009. “Tracking the roots of cellulase hyperproduction by the fungus *Trichoderma reesei* using massively parallel DNA sequencing *Proc Natl Acad Sci U S A*.” Published online before print September 2, 2009, doi:10.1073/pnas.0905848106.

Martinez D, RM Berka, B Henrissat, M Saloheimo, M Arvas, SE Baker, J Chapman, O Chertkov, PM Coutinho, D Cullen, EGJ Danchin, IV Grigoriev, P Harris, M Jackson, CP Kubicek, CS Han, I Ho, LF Larrondo, AL de Leon, JK Magnuson, S Merino, M Misra, B Nelson, N Putnam, B Robbertse, AA Salamov, M Schmoll, A Terry, N Thayer, A Westerholm-Parvinen, CL Schoch, J Yao, R Barbote, MA Nelson, C Detter, D Bruce, CR Kuske, G Xie, P Richardson, DS Rokhsar, SM Lucas, EM Rubin, N Dunn-Coleman, M Ward, and TS Brettin. 2008. “Genome sequencing and analysis of the biomass-degrading fungus *Trichoderma reesei* (syn. *Hypocrea jecorina*).” *Nature Biotechnology* 26(5):553-560.

Panisko EA, I Grigoriev, DS Daly, B-J Webb-Robertson, and SE Baker. 2009. “Genomes to Proteomes.” In: *Automation in Genomics and Proteomics: An Engineering Case-Based Approach*. G Alterovitz, M Ramoni, and RM Benson (eds.). Wiley, West Sussex.

Panisko EA, I Grigoriev, DS Daly, B-J Webb-Robertson, and SE Baker. 2009 “Genomes to Proteomes.” In *Automation in Genomics and Proteomics: An Engineering Case-Based Approach*. G Alterovitz, M Ramoni, and RM Benson (eds.). Wiley, West Sussex.

Shary S, AN Kapich, EA Panisko, JK Magnuson, D Cullen, and KE Hammel. 2008. “Differential Expression in *Phanerochaete chrysosporium* of Membrane-Associated Proteins Relevant to Lignin Degradation.” *Appl. Environ. Microbiol.* 74:7252-7257.

Thykaer J, MR Andersen, and SE Baker. 2009. “Essential pathway identification: from in silico analysis to potential antifungal targets in *Aspergillus fumigatus*.” *Med Mycol.*, 47 Suppl 1:S80-7. Epub 2009 Feb 27. PubMed PMID: 19253142.

Tsang A, G Butler, J Powlowski, EA Panisko, and SE Baker. 2009 “Analytical and Computational Approaches to Define the *Aspergillus niger* Secretome.” *Fungal Genetics and Biology*. 46 S1, 1563-160.

Wright JC, D Sugden, S Francis-McIntyre, I Riba-Garcia, SJ Gaskell, IV Grigoriev, SE Baker, RJ Beynon, and SJ Hubbard. 2009. “Exploiting proteomic data for genome annotation and gene model validation in *Aspergillus niger*.” *BMC Genomics*. Feb 4;10:61. PubMed PMID: 19193216; PubMed Central PMCID: PMC2644712.

Zhou K, EA Panisko, JK Magnuson, SE Baker, and I Grigoriev. 2009. “Proteomics for Validation of Automated Gene Model Predictions.” *Methods Mol. Biol.* 492:447-452.

Appendix A

Complete Analysis Report

Appendix A: Complete Analysis Report

JGI ID	No Mn pH 4.5	No Mn pH 5.0	No Mn pH 5.5	Mn pH 4.5	Mn pH 5.0	Mn pH 5.5	Blast Score	Blast eValue	Blast Hit Name	Hit Description	Species
206688	28	135	405	25	91	379	1929	0	RL3_ASPFU	60S ribosomal protein L3	<i>A. fumigatus</i>
209168	187	305	386	181	169	418	3784	0	CHL1_ASPNC	ATP-dependent RNA helicase chl1	<i>A. niger</i>
55586	16	35	262	7	16	274	1643	0	ALF_ASPOR	Fructose-bisphosphate aldolase	<i>A. oryzae</i>
212044	7	6	195	10	6	236	1305	1E-143	ADT_NEUCR	ADP,ATP carrier protein	<i>N. crassa</i>
199998	1	19	190		12	195	510	3E-51	COX4_NEUCR	Cytochrome c oxidase polypeptide 4, mitochondrial	<i>N. crassa</i>
52600	19	206	141	19	117	155	1292	1E-141	DCE1_ARATH	Glutamate decarboxylase 1	<i>A. thaliana</i>
180126	1	22	133		10	158	802	1E-84	HEX1_EMENI	Woronin body major protein	<i>E. nidulans</i>
54616		26	132	2	12	143	880	8E-94	ILV6_YEAST	Acetolactate synthase small subunit, mitochondrial	<i>S. cerevisiae</i>
208547		4	128		3	160	2788	0	ACL1_NEUCR	Probable ATP-citrate synthase subunit 1	<i>N. crassa</i>
53301	1	11	128	3	8	136			-No-Hit-	No Matching Hit found	
200483		14	127	4	6	174	1928	0	ACT_BOTFU	Actin	<i>B. fuckeliana</i>
54217	2	4	123	1	2	129			-No-Hit-	No Matching Hit found	
53274			109			108			-No-Hit-	No Matching Hit found	
210029	1	5	100		2	123	738	3E-77	EF1G2_YEAST	Elongation factor 1-gamma 2	<i>S. cerevisiae</i>
204461	10	16	98	7	10	119	1079	1E-117	RL2_ASHGO	60S ribosomal protein L2	<i>A. gossypii</i>
199133	2		78	2		97	1925	0	6PGD1_YEAST	6-phosphogluconate dehydrogenase, decarboxylating 1	<i>S. cerevisiae</i>
199043		3	66		6	73	1425	1E-157	ACL2_SCHPO	Probable ATP-citrate synthase subunit 2	<i>S. pombe</i>
214270	1	4	63	1	2	64	1402	1E-154	AATM_MOUSE	Aspartate aminotransferase, mitochondrial	<i>M. musculus</i>
206816		3	60		2	82	3609	0	EF2_NEUCR	Elongation factor 2	<i>N. crassa</i>
209716			60			74	820	2E-87	SODC_ASPNC	Superoxide dismutase [Cu-Zn]	<i>A. niger</i>
208343	1	4	55		3	60	1857	0	SAHH_YEAST	Adenylylhomocysteinase	<i>S. cerevisiae</i>
56247			53			52	856	2E-90	SPO14_YEAST	Phospholipase D1	<i>S. cerevisiae</i>
51717		7	51	2	1	74	859	2E-91	MPCP_YEAST	Mitochondrial phosphate carrier protein	<i>S. cerevisiae</i>
55611		1	51			60	944	1E-101	IF2A_SCHPO	Eukaryotic translation initiation factor 2 subunit alpha	<i>S. pombe</i>
197949	11	38	49	15	31	59	567	4E-58	RL21A_SCHPO	60S ribosomal protein L21-A	<i>S. pombe</i>
210867	14	70	49	13	49	50	374	2E-35	RL13_CANAL	60S ribosomal protein L13	<i>C. albicans</i>
52362		3	47		1	61	924	5E-99	RS0_NEUCR	40S ribosomal protein S0	<i>N. crassa</i>
54488		31	47		17	48			-No-Hit-	No Matching Hit found	
213187			46			72	4902	0	CLH_SCHPO	Probable clathrin heavy chain	<i>S. pombe</i>
56462		3	46		3	65	1940	0	GLYC_NEUCR	Serine hydroxymethyltransferase, cytosolic	<i>N. crassa</i>
209386	2	10	44		6	49	647	2E-67	RS11_YEAST	40S ribosomal protein S11	<i>S. cerevisiae</i>

JGI ID	No Mn pH 4.5	No Mn pH 5.0	No Mn pH 5.5	Mn pH 4.5	Mn pH 5.0	Mn pH 5.5	Blast Score	Blast eValue	Blast Hit Name	Hit Description	Species
55040		7	42		2	35	619	8E-64	SODM_ARATH	Superoxide dismutase [Mn], mitochondrial	<i>A. thaliana</i>
214348			39		1	41	3295	0	ACSA_EMENI	Acetyl-coenzyme A synthetase	<i>E. nidulans</i>
210514	1	4	38		2	54	1071	1E-116	IF3EI_DANRE	Eukaryotic translation initiation factor 3 subunit	<i>D. rerio</i>
196714	3	29	38	3	7	38	948	1E-102	RL15_ASPNG	60S ribomal protein L15	<i>A. niger</i>
212096		2	38		1	32	2280	0	EF1A_ASPOR	Elongation factor 1-alpha	<i>A. oryzae</i>
52269			37			46	1661	0	EIF3X_SCHPO	Probable eukaryotic translation initiation factor subunit	<i>S. pombe</i>
208387		12	37		11	33	229	7E-18	YLA3_SCHPO	Uncharacterized HTH La-type RNA-binding protein	<i>S. pombe</i>
214397		4	35		2	51	273	3E-23	AAT_AQUAE	Aspartate aminotransferase	<i>A. aeolicus</i>
118704			35			40	430	1E-40	YHKC_SCHPO	Uncharacterized aminotransferase C660.12c	<i>S. pombe</i>
139271			34			40	2182	0	GFA1_YEAST	Glucamine--fructe-6-phphate aminotransferase	<i>S. cerevisiae</i>
36287		1	34		1	32	605	2E-62	IF5A_CANAL	Eukaryotic translation initiation factor 5A	<i>C. albicans</i>
56891	1		33			40	1863	0	SYEC_SCHPO	Probable glutamyl-tRNA synthetase, cytoplasmic	<i>S. pombe</i>
55618			33			39	1303	1E-143	FPPS_GIBFU	Farnesyl pyrophosphate synthetase	<i>G. fujikuroi</i>
51912		1	32			50	1400	1E-154	ARLZ_SCHPO	Probable argininuccinate lyase	<i>S. pombe</i>
207206		5	32			37	829	8E-88	KTR1_YEAST	Alpha-1,2 mannyltransferase KTR1	<i>S. cerevisiae</i>
202152	7	27	32	7	6	33	491	4E-49	RL19B_SCHPO	60S ribomal protein L19-B	<i>S. pombe</i>
198713			31			41	1670	0	SSD1_YEAST	Protein SSD1	<i>S. cerevisiae</i>
53525		10	31		3	34	534	2E-54	RL32_NEUCR	60S ribomal protein L32	<i>N. crassa</i>
52554			30			48	3422	0	SYLC_NEUCR	Leucyl-tRNA synthetase, cytoplasmic	<i>N. crassa</i>
55644		6	30		2	41	807	9E-86	RS9_PODAN	40S ribomal protein S9	<i>P. anserina</i>
206105			30			38	1699	0	EIF3A_SCHPO	Probable eukaryotic translation initiation factor subunit	<i>S. pombe</i>
36448			30			26	127	1E-6	BTK_HUMAN	Tyrine-protein kinase BTK	<i>H. sapiens</i>
202416		1	29		1	50	880	6E-94	RS3_SCHPO	40S ribomal protein S3	<i>S. pombe</i>
56195			29		1	45	1971	0	COPG_SCHPO	Probable coatomer subunit gamma	<i>S. pombe</i>
202202			28			38	2098	0	FIMB_YEAST	Fimbrin	<i>S. cerevisiae</i>
173627		64	28		36	31	715	8E-75	UREG_ANADF	Urease accessory protein ureG	<i>Anaeromyxobacter sp.</i>
56836		1	28			30	999	1E-108	RHOA_EMENI	GTP-binding protein rhoA	<i>E. nidulans</i>
199485		14	28		8	30	257	2E-22	ATPK_SCHPO	ATP synthase subunit f, mitochondrial	<i>S. pombe</i>
56548			28			26	1361	1E-149	ERG6_NEUCR	Sterol 24-C-methyltransferase	<i>N. crassa</i>
124929			28			25	309	1E-27	MPPD1_MOUSE	Metallophosphoesterase domain-containing protein 1	<i>M. musculus</i>
208481			27			45	1906	0	SYMC_YEAST	Methionyl-tRNA synthetase, cytoplasmic	<i>S. cerevisiae</i>
205706			27			38	1378	1E-151	SPM1_SCHPO	Mitogen-activated protein kinase spm1	<i>S. pombe</i>
198674		1	27			29	882	2E-94	RL10A_NEUCR	60S ribomal protein L10a	<i>N. crassa</i>
52756			27			28	2338	0	COPB_SCHPO	Coatomer subunit beta	<i>S. pombe</i>

JGI ID	No Mn pH 4.5	No Mn pH 5.0	No Mn pH 5.5	Mn pH 4.5	Mn pH 5.0	Mn pH 5.5	Blast Score	Blast eValue	Blast Hit Name	Hit Description	Species
199495		1	26			49	1072	1E-116	RS4A_SCHPO	40S ribomal protein S4-A	<i>S. pombe</i>
52961			26			25	266	2E-22	PCBP3_HUMAN	Poly(rC)-binding protein 3	<i>H. sapiens</i>
198893			26			21	308	6E-27	PBP1_YEAST	PAB1-binding protein 1	<i>S. cerevisiae</i>
56136			24			27	1331	1E-146	AMPM1_SCHPO	Probable methionine aminopeptidase 1	<i>S. pombe</i>
199481			24			18	566	1E-57	NDUS4_NEUCR	NADH-ubiquinone oxidoreductase subunit, mitochondrial	<i>N. crassa</i>
208201			23			39	899	2E-96	ARF_AJECA	ADP-ribylation factor	<i>A. capsulata</i>
55252			23			37	968	1E-104	RS5_NEUCR	40S ribomal protein S5	<i>N. crassa</i>
202811			23			34	2553	0	HSP90_PODAN	Heat shock protein 90 homolog	<i>P. anserina</i>
49311		25	23		23	26			-No-Hit-	No Matching Hit found	
174332			23			16	132	7E-7	ZN341_HUMAN	Zinc finger protein 341	<i>H. sapiens</i>
182560			22			38	647	3E-66	IMB5_SCHPO	Importin subunit beta-5	<i>S. pombe</i>
197593			22			33			-No-Hit-	No Matching Hit found	
210935			22			28	1672	0	EIF3C_SCHPO	Probable eukaryotic translation initiation factor 3 subunit	<i>S. pombe</i>
207376			22			24	1109	1E-120	EIF3I_SCHPO	Eukaryotic translation initiation factor 3 39 kDa subunit	<i>S. pombe</i>
199503	14	20	22	16	13	24	478	6E-48	RL37_EMENI	60S ribomal protein L37	<i>E. nidulans</i>
196275			22			18	1562	1E-173	GBLP_NEUCR	Guanine nucleotide-binding protein subunit beta-like	<i>N. crassa</i>
203758			21			35	2009	0	DHE4_PENCH	NADP-specific glutamate dehydrogenase	<i>P. chrysogenum</i>
51711			21			27	1257	1E-137	PURA_SCHPO	Adenyluccinate synthetase	<i>S. pombe</i>
52676			21			25	1265	1E-138	RL5_NEUCR	60S ribomal protein L5	<i>N. crassa</i>
196044		1	21			22	820	3E-87	RL17_ASPFU	60S ribomal protein L17	<i>A. fumigatus</i>
53563			20			29	1206	1E-131	ENOF1_HUMAN	Mitochondrial enolase superfamily member 1	<i>H. sapiens</i>
56775		4	20			19	1784	0	ARP3_NEUCR	Actin-related protein 3	<i>N. crassa</i>
210558			20			19	2143	0	ILVB_YEAST	Acetolactate synthase catalytic subunit, mitochondrial	<i>S. cerevisiae</i>
183753			20			15	728	3E-76	GCY_YEAST	Protein GCY	<i>S. cerevisiae</i>
206681			20			14	1568	1E-173	CREA_ASPNG	DNA-binding protein creA	<i>A. niger</i>
55422		1	19			31	3872	0	SEC23_ASPNC	Protein transport protein sec23	<i>A. niger</i>
201401			19			29	872	4E-93	RL7_NEUCR	60S ribomal protein L7	<i>N. crassa</i>
206038			19			24	633	2E-65	ALTA7_ALTAL	Minor allergen Alt a 7	<i>A. alternata</i>
201439		1	19			20	788	6E-83	YOI1_SCHPO	Uncharacterized J domain-containing protein	<i>S. pombe</i>
212837		10	18		6	29	1795	0	UGPA1_SCHPO	Probable UTP--gluce-1-phphate uridylyltransferase	<i>S. pombe</i>
214104		1	18			25	1094	1E-118	KHSE_YEAST	Homerine kinase	<i>S. cerevisiae</i>
214112			18			16	1827	0	CBF5_ASPFU	Centromere/microtubule-binding protein cbf5	<i>A. fumigatus</i>
192720			17			32	925	8E-99	YCFD_SCHPO	UPF0364 protein C1393.13	<i>S. pombe</i>

JGI ID	No Mn pH 4.5	No Mn pH 5.0	No Mn pH 5.5	Mn pH 4.5	Mn pH 5.0	Mn pH 5.5	Blast Score	Blast eValue	Blast Hit Name	Hit Description	Species
205400			17			27	1972	0	IMB1_SCHPO	Importin subunit beta-1	<i>S. pombe</i>
189367			17			20	1385	1E-152	LAC2_BOTFU	Laccase-2	<i>B. fuckeliana</i>
130307			17			20	669	6E-69	BRX1_YEAST	Ribome biogenesis protein BRX1	<i>S. cerevisiae</i>
52803	2	6	17	5	2	15	863	7E-92	ODC2_YEAST	Mitochondrial 2-oxodicarboxylate carrier 2	<i>S. cerevisiae</i>
196131			17			13	168	1E-11	ATPN_YEAST	ATP synthase subunit g, mitochondrial	<i>S. cerevisiae</i>
209058			16			34	2806	0	MET3_ASPNG	Sulfate adenylyltransferase	<i>A. niger</i>
52388			16			29	2201	0	VPS1_SCHPO	Vacuolar protein sorting-associated protein 1	<i>S. pombe</i>
206944		16	16		7	23	341	6E-32	UBIQ_CANAL	Ubiquitin	<i>C. albicans</i>
46314			16			21	3723	0	YD22_SCHPO	Uncharacterized protein C56F8.02	<i>S. pombe</i>
51703			16			19	401	6E-38	PP2C4_SCHPO	Protein phosphatase 2C homolog 4	<i>S. pombe</i>
183233			16			17	1459	1E-160	THRC_SCHPO	Threonine synthase	<i>S. pombe</i>
128861			16			15	1023	1E-109	ACD11_CHICK	Acyl-CoA dehydrogenase family member 11	<i>G. gallus</i>
197796	1		15	1		24			-No-Hit-	No Matching Hit found	
208263			15			22	2195	0	TBB_ASPOR	Tubulin beta chain	<i>A. oryzae</i>
128750			15			21	861	1E-90	YCKC_SCHPO	PX domain-containing protein C1450.12	<i>S. pombe</i>
52878			15			19	197	2E-14	NAB2_YEAST	Nuclear polyadenylated RNA-binding protein NAB2	<i>S. cerevisiae</i>
49729			15			19	659	5E-68	SCJ1_YEAST	DnaJ-related protein SCJ1	<i>S. cerevisiae</i>
208051			15			18	1289	1E-141	IDH2_SCHPO	Isocitrate dehydrogenase [NAD] subunit 2, mitochondrial	<i>S. pombe</i>
174236		1	15			18			-No-Hit-	No Matching Hit found	
214233			15			17	5122	0	AGLU_ASPNG	Alpha-glucidase	<i>A. niger</i>
213140			15			17	1001	1E-107	SAC1_YEAST	Phosphoinositide phosphatase SAC1	<i>S. cerevisiae</i>
199078			15			15	285	1E-24	MTAD_METS3	5-methylthioadenine/S-adenylhomocysteine deaminase	<i>M. smithii</i>
187248	1		15			15	1731	0	2AAA_SCHPO	Protein phosphatase PP2A regulatory subunit A	<i>S. pombe</i>
181698			14			26	1673	0	YNR7_SCHPO	Uncharacterized protein C11G11.07	<i>S. pombe</i>
56871			14			17	1037	1E-112	YHM2_YEAST	Mitochondrial DNA replication protein YHM2	<i>S. cerevisiae</i>
52880			14			17	1714	0	UBR1_SCHPO	E3 ubiquitin-protein ligase ubr1	<i>S. pombe</i>
51819			14			16	1999	0	SYTC_SCHPO	Threonyl-tRNA synthetase, cytoplasmic	<i>S. pombe</i>
42169			14			14	561	5E-57	LAMB_EMENI	Lactam utilization protein lamB	<i>E. nidulans</i>
178461	1	12	14		8	11	770	1E-80	YAC2_SCHPO	Uncharacterized protein C16C9.02c	<i>S. pombe</i>
52441			14			8	1749	0	TCPD_SCHPO	T-complex protein 1 subunit delta	<i>S. pombe</i>
57091			14			6	1863	0	ASNS_SCHPO	Probable asparagine synthetase [glutamine-hydrolyzing]	<i>S. pombe</i>
52642			13			24	3374	0	SYIC_SCHPO	Isoleucyl-tRNA synthetase, cytoplasmic	<i>S. pombe</i>
56469			13			22	3386	0	COPA_SCHPO	Putative coatomer subunit alpha	<i>S. pombe</i>

JGI ID	No Mn pH 4.5	No Mn pH 5.0	No Mn pH 5.5	Mn pH 4.5	Mn pH 5.0	Mn pH 5.5	Blast Score	Blast eValue	Blast Hit Name	Hit Description	Species
56715			13			21	7228	0	ACAC_SCHPO	Acetyl-CoA carboxylase	<i>S. pombe</i>
198959			13			17	599	1E-61	RL9B_YEAST	60S ribomal protein L9-B	<i>S. cerevisiae</i>
202504		3	13		4	16	721	4E-76	RS19_EMENI	40S ribomal protein S19	<i>E. nidulans</i>
52474			13			13	1079	1E-116	NRD1_SCHPO	Negative regulator of differentiation 1	<i>S. pombe</i>
197079			13			13			-No-Hit-	No Matching Hit found	
56312			13			12	178	2E-12	WVOX_CHICK	WW domain-containing oxidoreductase	<i>G. gallus</i>
47873			13			12	1903	0	SYKC_SCHPO	Lysyl-tRNA synthetase, cytoplasmic	<i>S. pombe</i>
171507		3	13			11	1019	1E-110	HIS8_SCHPO	Histidinol-phosphate aminotransferase	<i>S. pombe</i>
45992			13			10	3830	0	CHSC_ASPFU	Chitin synthase C	<i>A. fumigatus</i>
119441			13			8			-No-Hit-	No Matching Hit found	
53726			13			7	181	2E-12	SFL1_YEAST	Flocculation suppression protein	<i>S. cerevisiae</i>
210782			12			23	174	3E-12	YA02_SCHPO	Uncharacterized protein C5H10.02c	<i>S. pombe</i>
57363			12			18	917	3E-97	PSME4_HUMAN	Proteasome activator complex subunit 4	<i>H. sapiens</i>
209010			12			15	921	2E-98	DHAS_SCHPO	Probable aspartate-semialdehyde dehydrogenase	<i>S. pombe</i>
205810			12			15	2060	0	CALX_ASPFU	Calnexin homolog	<i>A. fumigatus</i>
56120			12		1	14			-No-Hit-	No Matching Hit found	
56390			12			13	1085	1E-117	AATC_SCHPO	Aspartate aminotransferase, cytoplasmic Putative serine hydroxymethyltransferase, mitochondrial	<i>S. pombe</i>
211700			12			12	1862	0	GLYM_NEUCR	Serine/threonine-protein phosphatase subunit delta isoform	<i>N. crassa</i>
47102			12			10	1554	1E-171	2A5D_HUMAN		<i>H. sapiens</i>
55693			12			6	433	9E-43	HNT1_YEAST	Hit family protein 1	<i>S. cerevisiae</i>
207105			11			17	1313	1E-143	YB2G_SCHPO	Uncharacterized protein C31F10.16	<i>S. pombe</i>
200845			11			15	516	5E-51	SPO14_YEAST	Phospholipase D1	<i>S. cerevisiae</i>
57431			11			14	1696	0	PYRG_NEUCR	CTP synthase	<i>N. crassa</i>
206881		1	11		3	14	843	7E-90	RS7_NEUCR	40S ribomal protein S7	<i>N. crassa</i>
206203			11			14	398	7E-38	DHSO_BACHD	Sorbitol dehydrogenase Cleavage and polyadenylation specificity factor subunit 5	<i>B. halodurans</i>
183952			11			11	590	3E-60	CPSF5_XENLA		<i>X. laevis</i>
182955			11			11			-No-Hit-	No Matching Hit found	
56526			11			10	943	1E-101	AFG1_YEAST	Protein AFG1	<i>S. cerevisiae</i>
46615		3	11			9	1470	1E-161	YCW2_YEAST	WD repeat-containing protein YCR072C	<i>S. cerevisiae</i>
201877			11			9	2522	0	HXKG_ASPNG	Glucokinase	<i>A. niger</i>
42881			11			7	555	5E-56	URH1_YEAST	Uridine nucleidase	<i>S. cerevisiae</i>
52248			10			27	1467	1E-161	GAD8_SCHPO	Serine/threonine-protein kinase gad8	<i>S. pombe</i>
214022			10			19	780	3E-82	ADK1_ARATH	Adenine kinase 1	<i>A. thaliana</i>

JGI ID	No Mn pH 4.5	No Mn pH 5.0	No Mn pH 5.5	Mn pH 4.5	Mn pH 5.0	Mn pH 5.5	Blast Score	Blast eValue	Blast Hit Name	Hit Description	Species
172591			10			18	1137	1E-123	DCUP_YEAST	Uroporphyrinogen decarboxylase	<i>S. cerevisiae</i>
55918			10			17	1802	0	PP2A1_EMENI	Serine/threonine-protein phosphatase PP2A catalytic subunit	<i>E. nidulans</i>
54362			10			16	1163	1E-126	SYWC_YEAST	Tryptophanyl-tRNA synthetase, cytoplasmic	<i>S. cerevisiae</i>
130008			10			15	1640	0	AAP1_YEAST	Alanine/arginine aminopeptidase	<i>S. cerevisiae</i>
46410			10			14	1076	1E-116	NOC2_YEAST	Nucleolar complex protein 2	<i>S. cerevisiae</i>
53120			10			13	1949	0	PMT2_YEAST	Dolichyl-phosphate-mannose-protein mannyltransferase 2	<i>S. cerevisiae</i>
38927			10			11	150	3E-09	YA03_SCHPO	Uncharacterized protein C5H10.03	<i>S. pombe</i>
212077			10			11	923	3E-98	AP3B1_CANFA	AP-3 complex subunit beta-1	<i>C. familiaris</i>
173656			10			11	1979	0	LIDS_GAEGR	Linoleate diol synthase	<i>G. graminis</i>
120745			10			10	540	4E-54	MCS4_SCHPO	Response regulator mcs4	<i>S. pombe</i>
53063			10			8	144	4E-09	YNV8_SCHPO	Uncharacterized protein C3H7.08c	<i>S. pombe</i>
47529			10			8	1062	1E-114	SPT20_HUMAN	Spermatogenesis-associated protein 20	<i>H. sapiens</i>
119127			10			8	168	1E-10	GP1_CHLRE	Vegetative cell wall protein gp1	<i>C. reinhardtii</i>
180613			10			6	3008	0	SEC7_YEAST	Protein transport protein SEC7	<i>S. cerevisiae</i>
210951			10			4	2647	0	GCSP_SCHPO	Putative glycine dehydrogenase, mitochondrial	<i>S. pombe</i>
50058			10			2	406	1E-38	TGTL_SCHPO	Queuine tRNA-ribyltransferase-like protein	<i>S. pombe</i>
35679			9			16	324	6E-29	NIRA_EMENI	Nitrogen assimilation transcription factor nirA	<i>E. nidulans</i>
205183	1		9			15	3688	0	CDC48_EMENI	Cell division control protein 48	<i>E. nidulans</i>
136122			9			15	196	1E-14	CBP3_YEAST	Protein CBP3, mitochondrial	<i>S. cerevisiae</i>
47739			9			14	286	5E-25	MOB2_YEAST	CBK1 kinase activator protein MOB2	<i>S. cerevisiae</i>
181434			9			13	2608	0	PP2B_ASPFU	Serine/threonine-protein phosphatase 2B catalytic subunit	<i>A. fumigatus</i>
55770			9			12	119	1E-5	ZN362_HUMAN	Zinc finger protein 362	<i>H. sapiens</i>
213652		1	9			12	705	4E-73	PK1_DICDI	Forkhead-associated domain-containing protein kinase	<i>D. discoideum</i>
198862			9			12	245	2E-20	YE11_SCHPO	Uncharacterized protein C1B3.18c	<i>S. pombe</i>
54201			9			11	982	1E-105	RPN6_SCHPO	Probable 26S proteasome regulatory subunit rpn6	<i>S. pombe</i>
53576			9		1	10	231	2E-19	RLA2_ASPFU	60S acidic ribosomal protein P2	<i>A. fumigatus</i>
40848			9			10	232	1E-18	AIFM2_HUMAN	Apoptosis-inducing factor 2	<i>H. sapiens</i>
212992			9			10	3429	0	ODO1_YEAST	2-oxoglutarate dehydrogenase E1 component, mitochondrial	<i>S. cerevisiae</i>
209956			9			10	1402	1E-154	GSK3_SCHPO	Protein kinase gsk3	<i>S. pombe</i>
190965			9			10	271	4E-23	YJIA_ECOLI	Uncharacterized GTP-binding protein yjiA	<i>E. coli</i>
49747		7	9		4	9	2056	0	STUA_EMENI	Cell pattern formation-associated protein stuA	<i>E. nidulans</i>
209660			9			7	130	2E-6	EP300_HUMAN	Histone acetyltransferase p300	<i>H. sapiens</i>
55430			9			6			-No-Hit-	No Matching Hit found	

JGI ID	No Mn pH 4.5	No Mn pH 5.0	No Mn pH 5.5	Mn pH 4.5	Mn pH 5.0	Mn pH 5.5	Blast Score	Blast eValue	Blast Hit Name	Hit Description	Species
36954		2	9			6	196	2E-14	YL8J_SCHPO	Zinc finger protein C25B8.19c	<i>S. pombe</i>
48253			9			2			-No-Hit-	No Matching Hit found	
38101			9			1	2538	0	TAO3_YEAST	Cell morphogenesis protein PAG1	<i>S. cerevisiae</i>
56295			8			22	1826	0	CSE1_YEAST	Importin alpha re-exporter	<i>S. cerevisiae</i>
55563			8			12	1313	1E-144	URIC_ASPFL	Uricase	<i>A. flavus</i>
212876	1	3	8		1	12	819	6E-87	RS2_YEAST	40S ribomal protein S2	<i>S. cerevisiae</i>
56606			8			11	271	6E-24	RM51_YEAST	54S ribomal protein L51, mitochondrial	<i>S. cerevisiae</i>
53687			8			10	406	4E-39	YLIJ_ECOLI	Uncharacterized GST-like protein yliJ	<i>E. coli</i>
56196			8			8	1298	1E-142	SYDC_YEAST	Aspartyl-tRNA synthetase, cytoplasmic	<i>S. cerevisiae</i>
43791			8			6	365	3E-34	YE16_SCHPO	Uncharacterized methyltransferase C1B3.06c	<i>S. pombe</i>
35307			8			4	1457	1E-160	ARGD_NEUCR	Acetylmethionine aminotransferase, mitochondrial	<i>N. crassa</i>
210170			8			1	1945	0	RGA1_SCHPO	Rho-type GTPase-activating protein 1	<i>S. pombe</i>
200308			7			17	3300	0	EF3_CANAL	Elongation factor 3	<i>C. albicans</i>
197883		1	7			14	2038	0	PMA2_SCHPO	Plasma membrane ATPase 2	<i>S. pombe</i>
47358			7			13	8477	0	UTP10_ASPNC	U3 small nucleolar RNA-associated protein 10	<i>A. niger</i>
207465			7			12	971	1E-103	YN8E_SCHPO	Pumilio domain-containing protein P35G2.14	<i>S. pombe</i>
181371			7			12	2651	0	HSP70_EMENI	Heat shock 70 kDa protein	<i>E. nidulans</i>
56424			7			10	840	2E-89	DPM1_HUMAN	Dolichol-phosphate mannyltransferase	<i>H. sapiens</i>
46621			7			10	3547	0	GDE_YEAST	Glycogen debranching enzyme	<i>S. cerevisiae</i>
55637			7			7	2464	0	DHSA_SCHPO	Probable succinate dehydrogenase subunit, mitochondrial	<i>S. pombe</i>
55469			7			7	565	1E-56	VPS52_SCHPO	Vacuolar protein sorting-associated protein 52 Probable ubiquitin fusion degradation protein	<i>S. pombe</i>
52997			7		1	7	1134	1E-122	YDE1_SCHPO	C12B10.01c	<i>S. pombe</i>
40551			7			7	839	5E-89	TOXG_COCCA	Alanine racemase TOXG	<i>C. carbonum</i>
202289			7			7	136	1E-7	YII1_SCHPO	Uncharacterized protein C139.01c	<i>S. pombe</i>
137752	3	3	7		1	7	640	2E-66	RL20_YEAST	60S ribomal protein L20	<i>S. cerevisiae</i>
57072			7			6	1776	0	IF2G_YEAST	Eukaryotic translation initiation factor 2 subunit gamma	<i>S. cerevisiae</i>
206125			7			6	1083	1E-117	MAS5_SCHPO	Mitochondrial protein import protein mas5 Uncharacterized WD repeat-containing protein	<i>S. pombe</i>
209509	3	7	7	2	4	5	463	1E-44	YDSB_SCHPO	C4F8.11 Uncharacterized WD repeat-containing protein	<i>S. pombe</i>
209509	3	7	7	2	4	5	463	1E-44	YDSB_SCHPO	C4F8.11	<i>S. pombe</i>
38370			7			4	1430	1E-157	AACS_CHICK	Acetoacetyl-CoA synthetase	<i>G. gallus</i>
132771			7			4	885	3E-94	PMM_SCHPO	Phosphomannomutase	<i>S. pombe</i>
206602			7			3	316	2E-28	TPIS2_RHILO	Triphosphate isomerase 2	<i>R. loti</i>

JGI ID	No Mn pH 4.5	No Mn pH 5.0	No Mn pH 5.5	Mn pH 4.5	Mn pH 5.0	Mn pH 5.5	Blast Score	Blast eValue	Blast Hit Name	Hit Description	Species
52614			7			2	337	1E-30	DHC24_HUMAN	24-dehydrocholesterol reductase	<i>H. sapiens</i>
207217			6			15	3070	0	GYS_NEUCR	Glycogen [starch] synthase	<i>N. crassa</i>
207705			6			12	847	6E-90	RPN9_SCHPO	Probable 26S proteasome regulatory subunit rpn9	<i>S. pombe</i>
52666			6			10	461	2E-44	NU184_SCHPO	Nucleoporin nup184	<i>S. pombe</i>
57311			6			9	1463	1E-161	SERA_YEAST	D-3-phosphoglycerate dehydrogenase 1	<i>S. cerevisiae</i>
55785			6			9	399	6E-38	RM03_YEAST	54S ribosomal protein L3, mitochondrial	<i>S. cerevisiae</i>
54566			6			9	1219	1E-133	SYYM_NEUCR	Tyryl-tRNA synthetase, mitochondrial	<i>N. crassa</i>
53690			6			9	448	4E-44	ARPC3_SCHPO	Actin-related protein 2/3 complex subunit 3	<i>S. pombe</i>
56145			6			8	2401	0	TPSB_ASPNG	Alpha,alpha-trehalose-phosphate synthase [UDP-forming] 2	<i>A. niger</i>
55738			6			8	10186	0	PYR1_EMENI	Protein pyrABCN	<i>E. nidulans</i>
54083			6			8			-No-Hit-	No Matching Hit found	
52883			6			8	914	8E-98	PSB5_YEAST	Proteasome component PRE2	<i>S. cerevisiae</i>
48257			6			8	896	1E-95	TFTE_BURCE	Maleylacetate reductase	<i>B. cepacia</i>
42464			6			7	654	4E-68	SSP1_NEUCR	Peptidyl-prolyl cis-trans isomerase ssp-1	<i>N. crassa</i>
209255			6			7	1095	1E-119	YHM1_YEAST	Putative mitochondrial carrier protein YHM1/SHM1	<i>S. cerevisiae</i>
208393			6			7			-No-Hit-	No Matching Hit found	
45754			6			6	1642	0	SYQ_SCHPO	Probable glutaminyl-tRNA synthetase	<i>S. pombe</i>
207660			6			6	9361	0	FKS1_ASPNG	1,3-beta-glucan synthase component FKS1	<i>A. niger</i>
171927			6			6	1500	1E-165	FET3_CANAL	Iron transport multicopper oxidase FET3	<i>C. albicans</i>
56635			6			5	1565	1E-173	RIR2_NEUCR	Ribonucleide-diphosphate reductase small chain	<i>N. crassa</i>
45634			6			2	384	9E-36	ANKH1_HUMA N	Ankyrin repeat and KH domain-containing protein 1	<i>H. sapiens</i>
172390		1	5		2	13	1019	1E-110	SODB_ASPNG	Superoxide dismutase [Mn], mitochondrial	<i>A. niger</i>
56049			5			9	995	1E-107	PSD12_BOVIN	26S proteasome non-ATPase regulatory subunit 12	<i>B. taurus</i>
211731			5			9	882	7E-94	YFH6_YEAST	Uncharacterized peptidase YFR006W	<i>S. cerevisiae</i>
209198			5			9	2110	0	DHH1_ASPNC	ATP-dependent RNA helicase dhh1	<i>A. niger</i>
207219			5			9	1639	0	NMT1_ASPPA	Protein NMT1 homolog	<i>A. parasiticus</i>
55011			5			7	2496	0	NDUV1_ASPNG	NADH-ubiquinone oxidoreductase subunit, mitochondrial	<i>A. niger</i>
53232		1	5			7	1446	1E-159	DLDH_SCHPO	Dihydrolipoyl dehydrogenase, mitochondrial	<i>S. pombe</i>
41311			5			7	1912	0	MU138_SCHPO	Putative zinc protease mug138	<i>S. pombe</i>
55365			5			6			-No-Hit-	No Matching Hit found	
55055		1	5			6	2194	0	SIP5_ASPOR	Protein sip5	<i>A. oryzae</i>
213185			5			6	5645	0	PYC_ASPNG	Pyruvate carboxylase	<i>A. niger</i>
207003			5			6	1698	0	LYS1_EMENI	Saccharopine dehydrogenase [NAD+, L-lysine-forming]	<i>E. nidulans</i>

JGI ID	No Mn pH 4.5	No Mn pH 5.0	No Mn pH 5.5	Mn pH 4.5	Mn pH 5.0	Mn pH 5.5	Blast Score	Blast eValue	Blast Hit Name	Hit Description	Species
207470			5			5	1481	1E-163	SYNC_YEAST	Asparaginyl-tRNA synthetase, cytoplasmic	<i>S. cerevisiae</i>
57102		5	5	1	4	4	3420	0	RIR1_NEUCR	Ribonucleide-diphphate reductase large chain	<i>N. crassa</i>
56817			5			4	1063	1E-115	ANM1_SCHPO	Probable protein arginine N-methyltransferase	<i>S. pombe</i>
38620			5			4	942	1E-100	YIJ1_YEAST	Uncharacterized protein YIL091C	<i>S. cerevisiae</i>
206025			5			4	905	9E-97	ARPC2_SCHPO	Actin-related protein 2/3 complex subunit 2	<i>S. pombe</i>
193777			5			4	5615	0	BRR2_SCHPO	Pre-mRNA-splicing factor brr2	<i>S. pombe</i>
192903			5			4	971	1E-104	CSN6_EMENI	COP9 signalome complex subunit 6	<i>E. nidulans</i>
198943			5			3	766	2E-80	PCY1_SCHPO	Probable choline-phphate cytidylyltransferase	<i>S. pombe</i>
52146			5			2	2678	0	TRP_NEUCR	Tryptophan synthase	<i>N. crassa</i>
207204			5			2	457	2E-45	COX6_NEUCR	Cytochrome c oxidase polypeptide 6, mitochondrial	<i>N. crassa</i>
53467			5			1			-No-Hit-	No Matching Hit found	
57277			4			15	722	5E-76	YOP1_ASPFU	Protein yop1	<i>A. fumigatus</i>
51987			4			12	1726	0	PP1_EMENI	Serine/threonine-protein phphatase PP1	<i>E. nidulans</i>
194077			4			11	2783	0	SYV_NEUCR	Valyl-tRNA synthetase, mitochondrial	<i>N. crassa</i>
56701			4			10	882	2E-94	RL10A_SCHPO	60S ribomal protein L10-A	<i>S. pombe</i>
212120			4			10	1244	1E-135	AGM1_CANAL	Phphoacetylglucamine mutase	<i>C. albicans</i>
47885			4			9	472	3E-47	YGL4_SCHPO	Uncharacterized protein C216.04c	<i>S. pombe</i>
56093			4			8	2499	0	CND1_SCHPO	Condensin complex subunit 1	<i>S. pombe</i>
210433			4			8	2575	0	G6PI_ASPOR	Gluce-6-phphate isomerase	<i>A. oryzae</i>
206692			4			8	1497	1E-165	PUR8_YEAST	Adenyluccinate lyase	<i>S. cerevisiae</i>
204050			4			8			-No-Hit-	No Matching Hit found	
202461		1	4			8	898	3E-96	RL16_NEUCR	60S ribomal protein L16	<i>N. crassa</i>
194752			4			8			-No-Hit-	No Matching Hit found	
212484			4			7	2098	0	HAT2_ASPOR	Histone acetyltransferase type B subunit 2	<i>A. oryzae</i>
54762			4			6	2137	0	AMPD_SCHPO	AMP deaminase	<i>S. pombe</i>
35734			4			6	957	1E-102	LKH1_SCHPO	Dual specificity protein kinase lkh1	<i>S. pombe</i>
209562			4			6	383	6E-37	RS20_SCHPO	40S ribomal protein S20	<i>S. pombe</i>
198350			4			6	3179	0	NCPR_ASPNG	NADPH--cytochrome P450 reductase	<i>A. niger</i>
189778			4			6	190	1E-14	YA044_YEAST	Uncharacterized bolaA-like protein YAL044W-A	<i>S. cerevisiae</i>
138621			4			6	2402	0	STT4_YEAST	Phphatidylinitol 4-kinase STT4	<i>S. cerevisiae</i>
55909			4			5	1163	1E-126	SPN2_SCHPO	Septin homolog spn2	<i>S. pombe</i>
44033			4			5	2354	0	APE2_YEAST	Aminopeptidase 2, mitochondrial	<i>S. cerevisiae</i>
213093			4			5	1800	0	RPN2_SCHPO	26S proteasome regulatory subunit rpn2	<i>S. pombe</i>
203669			4			5	2365	0	METE_SCHPO	Probable homocysteine methyltransferase	<i>S. pombe</i>

JGI ID	No Mn pH 4.5	No Mn pH 5.0	No Mn pH 5.5	Mn pH 4.5	Mn pH 5.0	Mn pH 5.5	Blast Score	Blast eValue	Blast Hit Name	Hit Description	Species
128777			4			5	6505	0	DOP1_EMENI	Protein dopey	<i>E. nidulans</i>
55511			4			4	7908	0	FAS2_PENPA	Fatty acid synthase subunit alpha	<i>P. patulum</i>
53927			4			4	867	3E-92	IP11_ASPOR	Pre-rRNA-processing protein ipi1	<i>A. oryzae</i>
213429			4			4	1258	1E-137	GSHR_NEUCR	Glutathione reductase	<i>N. crassa</i>
56454			4			3	1470	1E-162	SIK1_SCHPO	Ribome biynthesis protein sik1	<i>S. pombe</i>
52653			4			3	1509	1E-166	PTPA2_ASPOR	Serine/threonine-protein phosphatase 2A activator 2	<i>A. oryzae</i>
38457			4			3	621	1E-63	VATC_YEAST	V-type proton ATPase subunit C	<i>S. cerevisiae</i>
179814			4			3	558	3E-56	SERB_SCHPO	Probable phosphatase	<i>S. pombe</i>
54781			4			2	289	4E-25	EIF3M_SCHPO	Eukaryotic translation initiation factor 3 subunit M	<i>S. pombe</i>
36569			4			2	1120	1E-121	VIP1_YEAST	Initol hexakisphosphate/diphosphoinitol-pentakisphosphate kinase	<i>S. cerevisiae</i>
191251			4			2	1486	1E-164	ALO_NEUCR	Putative D-arabinono-1,4-lactone oxidase	<i>N. crassa</i>
183352			4			2	622	1E-63	NHG1_PSEPU	Salicylate hydroxylase	<i>P. putida</i>
52774			4			1	2550	0	HTS1_COCCA	HC-toxin synthetase	<i>C. carbonum</i>
38814			4				184	1E-12	SSR4_SCHPO	SWI/SNF and RSC complexes subunit ssr4	<i>S. pombe</i>
142854			4				137	7E-08	Y4213_ARATH	UPF0480 protein At4g32130	<i>A. thaliana</i>
214140			3			13	3445	0	MYO2_SACKL	Myo-2	<i>S. kluyveri</i>
208510			3			8	3446	0	XPO1_SCHPO	Exportin-1	<i>S. pombe</i>
202623			3			7	939	1E-100	YDQD_SCHPO	Uncharacterized protein C5D6.13	<i>S. pombe</i>
176760			3			7	5276	0	NM111_ASPNC	Pro-apoptotic serine protease nma111	<i>A. niger</i>
56425			3			6	1347	1E-147	VPS35_SCHPO	Vacuolar protein sorting-associated protein 35	<i>S. pombe</i>
48994			3			6	2074	0	NOT1_SCHPO	General negative regulator of transcription subunit 1	<i>S. pombe</i>
36874			3	1		6	1236	1E-135	KAPB_YEAST	cAMP-dependent protein kinase type 2	<i>S. cerevisiae</i>
129080			3			6	3462	0	SF3B1_MOUSE	Splicing factor 3B subunit 1	<i>M. musculus</i>
54890			3			5	2320	0	CARA_ASPNC	Carbamoyl-phosphate synthase arginine-specific small chain	<i>A. niger</i>
214511			3			5	1470	1E-162	CSK2A_NEUCR	Casein kinase II subunit alpha	<i>N. crassa</i>
213627			3			5	1986	0	DNM1_YEAST	Dynamin-related protein DNM1	<i>S. cerevisiae</i>
208165			3			5	1643	0	LCB2_SCHPO	Serine palmitoyltransferase 2	<i>S. pombe</i>
200934			3			5	2005	0	IMA3_SCHPO	Probable importin c550.11	<i>S. pombe</i>
184284			3			5			-No-Hit-	No Matching Hit found	
56298			3			4	1811	0	GCS1_SCHPO	Probable mannyl-oligaccharide glucidase	<i>S. pombe</i>
55402			3			4	883	2E-93	YDHE_SCHPO	Pumilio domain-containing protein C6G9.14	<i>S. pombe</i>
40314			3			4	316	2E-28	YC4C_SCHPO	UPF0363 protein C1672.12c	<i>S. pombe</i>
209784		1	3			4	1175	1E-127	CMC1_MOUSE	Calcium-binding mitochondrial carrier protein Aralar1	<i>M. musculus</i>

JGI ID	No Mn pH 4.5	No Mn pH 5.0	No Mn pH 5.5	Mn pH 4.5	Mn pH 5.0	Mn pH 5.5	Blast Score	Blast eValue	Blast Hit Name	Hit Description	Species
211677	2	5	3	3	1	3	519	1E-52	RL44_PICJA	60S ribomal protein L44	<i>P. jadinii</i>
176640			3			3	148	1E-08	YN25_SCHPO	Uncharacterized transcriptional regulatory protein C530.05	<i>S. pombe</i>
171085			3			3	369	4E-34	ARP9_SCHPO	SWI/SNF and RSC complexes subunit arp9	<i>S. pombe</i>
204582			3			2			-No-Hit-	No Matching Hit found	
193773			3			2	2871	0	U5S1_CHICK	116 kDa U5 small nuclear ribonucleoprotein component	<i>G. gallus</i>
191914			3			2	334	2E-30	ACADL_MOUSE	Long-chain specific acyl-CoA dehydrogenase, mitochondrial	<i>M. musculus</i>
206102		17	3		10	1	474	6E-46	SNT2_SCHPO	Lid2 complex component snt2	<i>S. pombe</i>
202783			3			1	874	2E-93	YPT1_NEUCR	GTP-binding protein ypt1	<i>N. crassa</i>
56222			3				524	6E-52	K0090_CHICK	Uncharacterized protein KIAA0090 homolog	<i>G. gallus</i>
55587			3				149	2E-08	YGVA_SCHPO	CUE domain-containing protein C354.10	<i>S. pombe</i>
52445			3						-No-Hit-	No Matching Hit found	
124156			3				1578	1E-174	FDH_EMENI	Probable formate dehydrogenase	<i>E. nidulans</i>
47658			2			9	235	3E-18	NU120_SCHPO	Nucleoporin nup120	<i>S. pombe</i>
52865			2			8			-No-Hit-	No Matching Hit found	
197350			2			8	596	1E-61	RS16_ASHGO	40S ribomal protein S16	<i>A. gossypii</i>
205755			2			7	908	2E-97	ERV25_ASPFU	Endoplasmic reticulum vesicle protein 25	<i>A. fumigatus</i>
55590			2			6	2626	0	PGM_ASPFU	Phosphoglucomutase	<i>A. fumigatus</i>
49499			2			6	170	3E-11	PAMO_THEFY	Phenylacetone monooxygenase	<i>T. fusca</i>
210814			2			6	741	5E-78	YPT2_SCHPO	GTP-binding protein ypt2	<i>S. pombe</i>
207011			2			6	889	1E-94	KES1_YEAST	Protein KES1	<i>S. cerevisiae</i>
200566			2			6	598	2E-61	NACA_ASPNC	Nascent polypeptide-associated complex subunit alpha	<i>A. niger</i>
52335			2			5	923	2E-98	ANM3_SCHPO	Ribomal protein arginine N-methyltransferase rmt3	<i>S. pombe</i>
209597			2			5	1417	1E-156	HHP1_SCHPO	Casein kinase I homolog hhp1	<i>S. pombe</i>
207707			2			5	1428	1E-157	NDUA9_NEUCR	NADH-ubiquinone oxidoreductase subunit, mitochondrial	<i>N. crassa</i>
203924			2			5	2159	0	SC61A_NEUCR	Protein transport protein SEC61 subunit alpha	<i>N. crassa</i>
52565			2			4	4180	0	SEC24_ASPNC	Protein transport protein sec24	<i>A. niger</i>
35776			2			4	554	1E-55	YEY6_SCHPO	Putative methyltransferase C2C4.06c	<i>S. pombe</i>
44220			2			3	241	4E-19	CL030_HUMAN	TPR repeat-containing protein C12orf30	<i>H. sapiens</i>
213437			2			3	915	1E-97	BGLA_BACCI	Beta-glucidase	<i>B. circulans</i>
211010			2			3	649	9E-67	DSK1_SCHPO	Protein kinase dsk1	<i>S. pombe</i>
210321			2			3	1678	0	IMA1_SCHPO	Importin subunit alpha-1	<i>S. pombe</i>
204865		1	2			3	405	4E-39	YHS2_YEAST	UPF0195 protein YHR122W	<i>S. cerevisiae</i>

JGI ID	No Mn pH 4.5	No Mn pH 5.0	No Mn pH 5.5	Mn pH 4.5	Mn pH 5.0	Mn pH 5.5	Blast Score	Blast eValue	Blast Hit Name	Hit Description	Species
199462			2			3	396	2E-38	RL261_ARATH	60S ribosomal protein L26-1	<i>A. thaliana</i>
185810		3	2			3			-No-Hit-	No Matching Hit found	
185582			2			3	921	3E-98	YC7C_SCHPO	Uncharacterized esterase/lipase C417.12	<i>S. pombe</i>
136079			2			3	820	6E-87	YFG5_SCHPO	Uncharacterized mitochondrial carrier C19G12.05	<i>S. pombe</i>
54759			2			2	281	6E-24	ELMO2_HUMA N	Engulfment and cell motility protein 2	<i>H. sapiens</i>
54540			2			2	1268	1E-138	AROF_NEUCR	Phpho-2-dehydro-3-deoxyheptonate aldolase	<i>N. crassa</i>
51860			2			2	513	2E-51	YJZ4_YEAST	Putative aldolase class 2 protein YJR024C	<i>S. cerevisiae</i>
49007			2			2	200	6E-15	FOL1_PNECA	Folic acid synthesis protein fol1	<i>P. carinii</i>
44948			2			2			-No-Hit-	No Matching Hit found	
44363			2			2	444	2E-42	NU132_SCHPO	Nucleoporin nup132	<i>S. pombe</i>
38174			2			2	1353	1E-148	RAV1_YEAST	Regulator of V-ATPase in vacuolar membrane protein 1	<i>S. cerevisiae</i>
211691			2			2	3565	0	GCN1_SCHPO	Translational activator gen1	<i>S. pombe</i>
206151			2			2	922	4E-99	SAR1_ASPNG	Small COPII coat GTPase SAR1	<i>A. niger</i>
190197			2			2	247	5E-20	DPF6_CAEEL	Dipeptidyl peptidase family member 6	<i>C. elegans</i>
180652			2			2			-No-Hit-	No Matching Hit found	
174315			2			2	2869	0	YM54_YEAST	Uncharacterized protein YMR196W	<i>S. cerevisiae</i>
137182			2			2	317	5E-29	RL14A_YEAST	60S ribosomal protein L14-A	<i>S. cerevisiae</i>
54451			2			1	1075	1E-116	UAP1_CANAL	UDP-N-acetylglucamine pyrophosphorylase	<i>C. albicans</i>
53297			2			1	1293	1E-141	SND1_SCHPO	Staphylococcal nuclease domain-containing protein 1	<i>S. pombe</i>
52578			2			1	860	2E-91	YAUB_SCHPO	UPF0012 hydrolase C26A3.11	<i>S. pombe</i>
51257			2			1	635	7E-65	NOP14_YARLI	Probable nucleolar complex protein 14	<i>Y. lipolytica</i>
50504			2			1	697	1E-72	ALDX_SPOSA	Aldehyde reductase 1	<i>S. salmonicolor</i>
46347			2			1			-No-Hit-	No Matching Hit found	
36938			2			1			-No-Hit-	No Matching Hit found	
196625			2			1	900	6E-96	YAI8_SCHPO	Uncharacterized protein C24B11.08c	<i>S. pombe</i>
196055			2			1			-No-Hit-	No Matching Hit found	
193747			2			1	532	2E-53	RCL1_SCHPO	Probable RNA 3'-terminal phosphate cyclase-like protein	<i>S. pombe</i>
181700			2			1	1098	1E-119	RPN11_SCHPO	26S proteasome regulatory subunit rpn11	<i>S. pombe</i>
143580			2			1	389	1E-37	RS10A_YEAST	40S ribosomal protein S10-A	<i>S. cerevisiae</i>
54281			2				1928	0	CYSD_EMENI	O-acetylhomoserine (thiol)-lyase	<i>E. nidulans</i>
51606			2				258	2E-21	RLM1_YEAST	Transcription factor RLM1	<i>S. cerevisiae</i>
47046			2				685	1E-71	ARF6_HUMAN	ADP-ribosylation factor 6	<i>H. sapiens</i>
40650			2				123	1E-5	YL278_YEAST	Uncharacterized transcriptional regulatory protein	<i>S. cerevisiae</i>

JGI ID	No Mn pH 4.5	No Mn pH 5.0	No Mn pH 5.5	Mn pH 4.5	Mn pH 5.0	Mn pH 5.5	Blast Score	Blast eValue	Blast Hit Name	Hit Description	Species
39468			2				416	5E-40	CIA30_NEUCR	Complex I intermediate-associated protein 30, mitochondrial	<i>N. crassa</i>
214686			2				1082	1E-117	OXDC_BACSU	Oxalate decarboxylase oxdC	<i>B. subtilis</i>
207730			2				920	1E-98	RL8_SCHPO	60S ribomal protein L8	<i>S. pombe</i>
170595			2				1207	1E-131	TAF5_SCHPO	Transcription initiation factor TFIID subunit 5	<i>S. pombe</i>
37620			1			9	3574	0	DHE2_NEUCR	NAD-specific glutamate dehydrogenase	<i>N. crassa</i>
181825			1			7	466	3E-45	NCBP1_YEAST	Nuclear cap-binding protein complex subunit 1	<i>S. cerevisiae</i>
40935			1			6	373	5E-35	PIP_BACCO	Proline iminopeptidase	<i>B. coagulans</i>
211159			1			6	2265	0	ATPB_NEUCR	ATP synthase subunit beta, mitochondrial	<i>N. crassa</i>
178053			1			6	444	6E-43	CP67_UROFA	Cytochrome P450 67 (Fragment)	<i>U. fabae</i>
56378			1			5			-No-Hit-	No Matching Hit found	
52396			1			4	804	1E-84	YE04_SCHPO	Uncharacterized RNA-binding protein C17H9.04c	<i>S. pombe</i>
48594			1			3	3859	0	SEPA_EMENI	Cytokinesis protein sepA	<i>E. nidulans</i>
44662			1			3	122	3E-6	FYV4_ASHGO	Protein FYV4, mitochondrial	<i>A. gossypii</i>
212902			1			3	522	4E-52	YHXB_SCHPO	Uncharacterized J domain-containing protein C3E7.11c	<i>S. pombe</i>
212470			1			3	2111	0	UBP21_SCHPO	Ubiquitin carboxyl-terminal hydrolase 21	<i>S. pombe</i>
208150			1			3	1260	1E-137	NDH1_SCHPO	Probable NADH-ubiquinone oxidoreductase, mitochondrial	<i>S. pombe</i>
206525			1			3	945	1E-101	SYYC_YEAST	Tyryl-tRNA synthetase, cytoplasmic	<i>S. cerevisiae</i>
197459			1			3	1023	1E-110	EIF3E_SCHPO	Eukaryotic translation initiation factor 3 subunit E	<i>S. pombe</i>
55763			1			2	1850	0	MPI_ASPFU	Manne-6-phphate isomerase	<i>A. fumigatus</i>
55041			1			2	2363	0	HSP75_CANAL	Heat shock protein SSB1	<i>C. albicans</i>
52748			1			2	479	1E-47	RL6B_YEAST	60S ribomal protein L6-B	<i>S. cerevisiae</i>
52431			1			2	522	3E-52	IF2B_SCHPO	Probable eukaryotic translation initiation factor 2 subunit	<i>S. pombe</i>
52249			1			2	2297	0	COPB2_HUMAN	Coatomer subunit beta'	<i>H. sapiens</i>
51182			1			2	3122	0	TOM1_NEUCR	E3 ubiquitin-protein ligase TOM1-like protein	<i>N. crassa</i>
48846			1			2	660	1E-67	SCC3_SCHPO	Cohesin subunit psc3	<i>S. pombe</i>
46294			1			2	1463	1E-161	PAP_SCHPO	Poly(A) polymerase pla1	<i>S. pombe</i>
214434			1			2	183	2E-12	CTF1A_FUSSO	Cutinase transcription factor 1 alpha	<i>F. solani</i>
213708			1			2	359	4E-33	YLP3_PSEPU	Uncharacterized methyltransferase in lpd-3 5'region	<i>P. putida</i>
202801			1			2	2253	0	CISY_ASPNG	Citrate synthase, mitochondrial	<i>A. niger</i>
200493			1			2	663	7E-69	HIS7_NEUCR	Imidazoleglycerol-phphate dehydratase	<i>N. crassa</i>
56096		3	1				1411	1E-154	PO152_SCHPO	Probable nucleoporin POM152-like	<i>S. pombe</i>
36909	1	17	1	3	8		140	2E-7	MUC1_BOVIN	Mucin-1	<i>B. taurus</i>
190014		2	1				1087	1E-117	WA_EMENI	Conidial yellow pigment biynthesis polyketide synthase	<i>E. nidulans</i>

JGI ID	No Mn pH 4.5	No Mn pH 5.0	No Mn pH 5.5	Mn pH 4.5	Mn pH 5.0	Mn pH 5.5	Blast Score	Blast eValue	Blast Hit Name	Hit Description	Species
119698		2	1				257	5E-21	ZDS1_SCHPO	Protein zds1	<i>S. pombe</i>
39005		1				4			-No-Hit-	No Matching Hit found	
56485	1						1656	0	G3P_ASPNG	Glyceraldehyde-3-phphate dehydrogenase	<i>A. niger</i>
56124	5	28			18	1	169	1E-10	YE38_SCHPO	Uncharacterized protein C20G4.08	<i>S. pombe</i>
49737		5				1			-No-Hit-	No Matching Hit found	
170608		3				1			-No-Hit-	No Matching Hit found	
56903	4			3			458	7E-45	IF4E2_MOUSE	Eukaryotic translation initiation factor 4E type 2	<i>M. musculus</i>
55964					2		1115	1E-121	HOT_BOVIN	Hydroxyacid-oxoacid transhydrogenase, mitochondrial	<i>B. taurus</i>
55859	2	21		1	16		2351	0	HRP3_SCHPO	Chromodomain helicase hrp3	<i>S. pombe</i>
54867	4	4		3	1				-No-Hit-	No Matching Hit found	
53737	3	2		2			759	2E-79	SCD2_SCHPO	Protein scd2/ral3	<i>S. pombe</i>
53632		22			16		178	8E-12	NSR1_YEAST	Nuclear localization sequence-binding protein	<i>S. cerevisiae</i>
53539		3					162	1E-10	YKH3_SCHPO	Uncharacterized protein PYUK71.03c DNA damage-responsive transcriptional repressor	<i>S. pombe</i>
52694		9			6		727	2E-75	RPH1_YEAST	RPH1	<i>S. cerevisiae</i>
49427		2					190	2E-13	EME1_SCHPO	Crsover junction endonuclease eme1	<i>S. pombe</i>
41302		3							-No-Hit-	No Matching Hit found	
39038		7			4				-No-Hit-	No Matching Hit found	
214402		2					310	8E-28	XFIN_XENLA	Zinc finger protein Xfin	<i>X. laevis</i>
210265	14	6		12	2		900	1E-95	GEPH_DICDI	Gephyrin	<i>D. discoideum</i>
209514		4			4		115	4E-5	MYB_XENLA	Myb protein	<i>X. laevis</i>
208244	8	13		12	8	8	1421	1E-156	KIN1_SCHPO	Protein kinase kin1	<i>S. pombe</i>
202206					3		1260	1E-137	PROA_SCHPO	Probable gamma-glutamyl phphate reductase	<i>S. pombe</i>
202087		2					1370	1E-150	NDE1_ASPFU	Nuclear distribution protein nudE homolog 1	<i>A. fumigatus</i>
190247		4			1				-No-Hit-	No Matching Hit found	
181863		2					5465	0	SEC16_ASPNC	COPII coat assembly protein sec16	<i>A. niger</i>
177822		20			8		318	7E-29	YN82_SCHPO	UPF0424 protein P35G2.02	<i>S. pombe</i>
174643		1			2		2774	0	SCONB_EMENI	Sulfur metabolite repression control protein	<i>E. nidulans</i>



Pacific Northwest
NATIONAL LABORATORY

902 Battelle Boulevard
P.O. Box 999
Richland, WA 99352
1-888-375-PNNL (7665)

www.pnl.gov



U.S. DEPARTMENT OF
ENERGY